Design and Signal Processing of Finger Photo Plethysmograph Ring Sensors for Reduced Motion Artifact and Circulation Interference

by

Reginald C. Hutchinson

B.S., Mathematics (1999)
Morehouse College

B.M.E., Engineering (1999)
The George W. Woodruff School of Mechanical Engineering
Georgia Institute of Technology

Submitted to the Department of Mechanical Engineering and the Department of Electrical Engineering and Computer Science in Partial Fulfillment of the Requirements for the Degrees of

Master of Science in Mechanical Engineering
and
Master of Science in Electrical Engineering and Computer Science
at the
Massachusetts Institute of Technology
May 2002 (June 2002)

Signature of Author_____
Department of Mechanical Engineering
May 24, 2002

Certified by_____
Haruhiko Harry Asada
Ford Professor of Mechanical Engineering
Thesis Supervisor

Accepted by_____
Ain A. Sonin
Chairman, Department Committee on Graduate Students
Department of Mechanical Engineering

Accepted by_____
Arthur C. Smith
Chairman, Committee on Graduate Students
Department of Electrical Engineering and Computer Science

Design and Signal Processing of Finger Photo Plethysmograph Ring Sensors for Reduced Motion Artifact and Circulation Interference

by

Reginald C. Hutchinson

Submitted to the Department of Mechanical Engineering and the Department of Electrical Engineering and Computer Science on May 20, 2002 in Partial Fulfillment of the Requirements for the Degrees of Master of Science in Mechanical Engineering and Master of Science in Electrical Engineering and Computer Science

ABSTRACT

This work centers on creating a new design for a photo plethysmograph ring sensors to address the problems of previous ring sensors. Two major issues are addressed: to improve the signal-to-noise ratio and lack of motion detection. A new design for photo plethysmographic devices is presented to increase the amplification of arterial volumetric pulsations. The unit provides a mechanism capable of pressurizing the finger base at localized point, thus circulation is not obstructed. An experiment study compares the new design with a cuff system. Results show that the new design does not obstruct the blood, while the cuff does. In addition, the new design will decrease corruption of the signal due to saturation effects from ambient light and small motion perturbation.

Motion detection was also presented in this work. Based on size and power constraints, an autocorrelation method in addition to a 2^{nd} photodetector (motion detector) were decided upon. The motion detector is more susceptible to motion, thus providing a noise reference. An algorithm using the autocorrelation method determines if motion is present based on the noise reference.

Thesis Supervisor: H. Harry Asada, Ph.D.
Ford Professor of Mechanical Engineering, Director, d'Arbeloff Laboratory for Information Systems and Technology

ACKNOWLEDGEMENTS

During my time at the Massachusetts Institute of Technology, I have encountered many trials and tribulations. Without the love and support from family and friends, these last few years would have been too overwhelming.

First of all, I would like to thank God for giving me not only the strength and endurance to fulfill my obligations, but for proving me with the mindset to undertake endure each obstacle and challenge in my life. Providing me with a continuous cast of friends, allowed my spirits never to be crushed.

I would like to thank my advisor, Professor Asada for his guidance, support and patience. These last years under his tutelage have strengthened my skills and provided me with additional knowledge which will last a lifetime.

I would like to thank my father. Besides being a role model everyday of my life, his continuous wisdom and unconditional love makes me grow closer each day to become half the man he is. I would like to acknowledge my mother, for her goodwill and nature provide me with a strong fundamental basis to withstand and endure challenges in my life. Inheriting her strong desires, and ability to burn the midnight oil which has been critical during this phase. Treasure, my twin sister, deserves recognition for always motivating me and inspiring me to reach my potential. She is definitely one of the most important people in my life who has been there for me and requires nothing in return. Thank you for always been so understanding and loving. You have been always been a great friend.

Then there is always Nishan, a brother to me since day one. No matter if he is in California or London, no matter if it is 4 p.m. or 4 a.m., he is always available for me to talk his head off. Thanks for being there. Crandall and Shane, two other friends that have never left my side. I am fortunate to have them in my life. Back then I never knew what I had when I had it. They have shown me what true friends are.

There are some organizations, which in need to acknowledge that have been a place support and a stress outlet. These organizations are: The Black Graduate Students Association, Graduate Student Council, BSU, and Greater Boston Morehouse College Alumni Association. In addition I would like to thank the Graduate Student Office who have provided counseling and guidance all throughout my stay. Dean Colbert, Dean Staton and Dean Charles have always gone above and beyond there duties to assist those in need. And to Mamma Leslie deserves thanks for taking time out of her busy life to help a young man out.

I would like to recognize ASADA GROUP for proving the lab place to be a good home. Outings, lab lunch and volleyball definitely make coming to work a little better. Also, they constantly show support and unselfishness by always willing to help someone else no matter their workload.

And lastly to Mike and Byron. Friends whom I came in with that have definitely shown that they will always be around to the end. My experience at MIT will always have them in memory.

And I have to special thanks to R.C. and the General. You have definitely helped me sustain my sanity.

CONTENTS

LIST OF FIGURES

LIST OF TABLES

CHAPTER 1
INTRODUCTION

1.1 Introduction

If new medical devices had increased functionality without compromising their accuracy, they may become commonplace in hospitals and other medical realms. Among the most common health monitoring instruments used in the medical arena are pulse oximeters. Pulse oximeters are medical devices used to monitor aspects of personal health, such as pulse rate and blood oxygen saturation level. Though devices such as ambulatory EKG monitoring devices have added the functionality of mobile monitoring, they place a load upon the individual. For long-term monitoring, this load can cause significant discomfort for the user. Other devices such as the FinaPres, noninvasive continuous finger blood pressure monitor, based on the vascular unloading technique, can monitor the patient, but have the potential to impede circulation throughout the finger [29].

The introduction of the photo plethysmographic device, termed the "new ring sensor" is a cost-effective complement that enables subjects to be monitored despite movement and without supervision by a medical professional. In addition, the use of this assistive monitoring equipment will aid medical facilities by improving a diagnostic tool that can help determine the status of the patient [10]. As such, this new device will make more efficient use of scarce health care workers. The equipment has been shown to meet various constraints including power consumption, weight, comfort, and accuracy.

Though this ring sensor has been shown to compare with other renowned devices such as EKG and other current FDA approved devices [19], several deficiencies persist. Also, the ring sensor has the potential to increase in its functionality thus becoming more durable.

The goal of this thesis is to develop a new ring sensor design to improve the signal-to-noise ratio my means of inducing a localized pressure at a point on the finger base without interfering with the blood circulation. A motion detection system will also be introduced to improve the performance of the ring sensor. Though these features will be provided, constraints and the performance of the original ring sensor will be met. In addition, the new design will decrease the corruption of the signal due to saturation effects from ambient light and small disturbances due to motion. Though, this framework is applicable to the ring sensor, it can be modified slightly such that other photo plethysmographic sensors can benefit from these findings.

1.2 Background

During the last century, many people experimented with photo plethysmography. This field was a highly active area of research in the development of non-invasive blood monitoring devices to aid the patient and provide a user-friendly apparatus to the medical professional using the equipment. From research involving ear photo plethysmographic devices in the 1940s [5], to Yamasitha's first analog photo plethysmograph sensor [19],

to the present day pulse oximeters, technology has shown great advancement. In addition, temperature and pressure effects have been observed with photo plethysmographic devices. It is observed that if heat were produced into the system, better circulation would result, providing a more reliable signal. Safety issues and regulations are considered to ensure that the heat is not uncomfortable to a patient. Pressure effects on a photo plethysmograph sensor have been investigated by use of various finger cuffs [21]. Important parameters, such as the blood pressure, were obtained using these devices. Others researchers observed the tradeoffs of using increased pressure to provide and accurate measurement. They accessed the state of how much pressure can be applied before serious complications can result [9].

The area of motion artifact has been a nuisance in producing and accessing the status of a patient. A motion artifact disrupts the signal to extent where it cannot be recovered. Because of the distorted waveform, it is difficult to capture certain physical characteristics. If motion can be detected, the sensor unit can take some action to ensure the data is reliable. Current pulse oximeters vary with this feature. Among those devices that contain this aspect, have an indicator to alert the user or medial professional. Though some devices indicate motion others attempt to eliminate motion. Though many people have committed extensive research to address the issue of motion artifact rejection such as Barreto and Vicente, it is still a highly thought of area of research since motion artifact still plagues many photo plethysmographic sensors [1]-[3]. If motion can be reduced or eliminated, prominent features can be extracted out of the measurement.

1.3 Outline of Thesis

This thesis focuses on how the new ring sensor design can solve key issues with the previous ring sensor and other photo plethysmographic devices. In addition, this new unit will improve the signal-to-noise ratio and establish a motion detection system. Chapter 2 begins this discussion by proving the reader previous information regarding the ring sensor, the theory in which it operates, and present issues with the previous ring sensor design and other photo plethysmographic devices. The next chapter, Chapter 3, goes on to provide a discussion on the new ring sensor design, operation of the unit, description of its components and their functionality, and resolution of issues as a result of the design. Chapter 4 focuses on the added functionality of signal-to-noise enhancement, while not impeding circulation to other essential parts of the finger. To show this improvement a comparison of localized point pressure and a uniform surface pressure are presented. Chapter 5 discusses the key issues with motion artifact. It investigates 4 key methods for motion detection: accelerometer, maximum likelihood method, autocorrelation technique, and an additional photodetector. It will evaluate the pros and cons of each method and based on the performance and abilities to meet current constraints, will decided the best method. Chapter 6 will describe the ring sensor monitoring system. Three additional sensors will be utilized for behavior and environmental monitoring. Chapter 7 will conclude this thesis with conclusions from this project and a list of recommendations for future improvement.

CHAPTER 2
REVIEW OF THE RING SENSOR

2.1 DESCRIPTION OF THE RING SENSOR

A brief description of the present ring sensor is reviewed in order to provide familiarity with the unit. The ring sensor is a miniature, low power continuous monitoring device. Encompassing the idea of pulse oximetry, it can provide important information about the wearer. The ring sensor uses two light-emitted diodes (LED) (660 nm and 940 nm) and a photodiode. If the sensor is wireless, then additional components are needed: a CPU, RF transmitter, and a battery unit. For purposes related to this research, concentration is placed on a wired ring sensor, such that the additional noise from the wireless network was not captured by the system. Whether wireless or wired, the ring sensor has the ability to modulate the two LEDs. The result, the signal-processing unit can monitor the arterial blood volume at the finger base. This information is transmitted to the host computer where further computations can yield the pulse rate and the arterial oxygen saturation level. In addition to calculating these parameters, the host computer serves as a data storage, and a means where the pulse waveform and the desired attributes can be displayed.

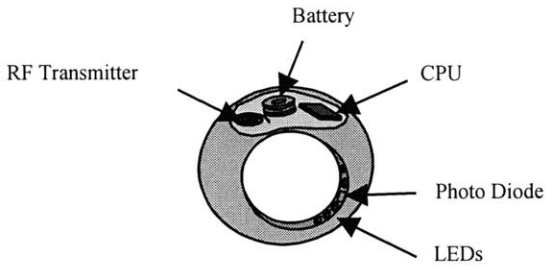

Figure 2.1 Conceptual diagram of the ring sensor [12]

The ring sensor uses both the theory of photo plethysmography and the knowledge of the dynamic wall in its design. The following sections will discuss these two ideas.

2.2 Theory of Photo Plethysmography

Photo plethysmography (PPG) is a method of measuring the cardiovascular pulse waveforms by optical means. Pulse oximetery uses photo plethysmography to measure the arterial oxygen saturation by a non-invasive spectrophotometric method [13]. Pulse oximeters are products in medical field which uses these theories to evaluate the pulse rate and the blood oxygen saturation level of an individual. Their ability to measure these parameters non-invasively makes them preferred by the public. Because of real-time monitoring capabilities and accuracy, they are commonplace in the hospitals and continuously used by medical professionals for initial diagnosis. Though many pulse

oximeters can differ in geometry, location on the body, and performance under different external factors, they all use the theory of photo plethysmography to obtain the pertinent information.

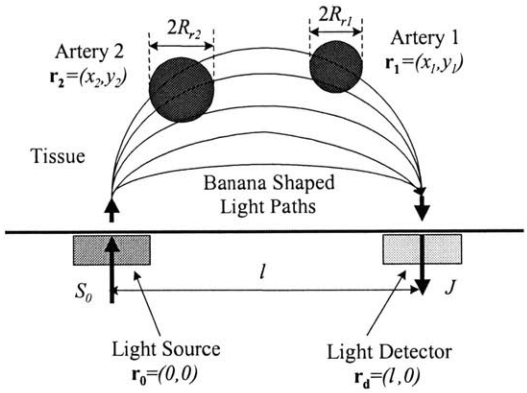

Figure 2.2 Optical model of the finger and optical elements. Blood vessels have different optical properties from the tissue. [12]

By using three components, two LEDs and a photodiode, the amount of blood volume can be measured. The photons from the LEDs pass through the skin. Although the photons illuminate in all directions, it is known that the average light path travels in a banana shape through a portion of the tissue and then back to the photodetector [19]. Although, some scattered light escapes through the finger, it will be assumed that the light emitted is absorbed solely by the anatomy of the finger and the photodetector. In light of this fact, Beer- Lambert's law can be applied to find the properties of amount of light absorbed.

$$I = I_o e^{-\varepsilon(\lambda)cd} \qquad (2.1)$$

,where I_o is the original intensity of the light, $\varepsilon(\lambda)$ is the extinction coefficient of absorbitivity at a specific wavelength λ, c is the concentration of the substance absorbing the light, and d is the optical path length. Certain have substances have shown to have a distinct spectrum when shined at different wavelengths [5]. Figure 2.2 shows the absorption spectrum for methaemoglobin, oxyhaemoglobin, deoyhaemoglobin, and carboxyhaemoglobin.

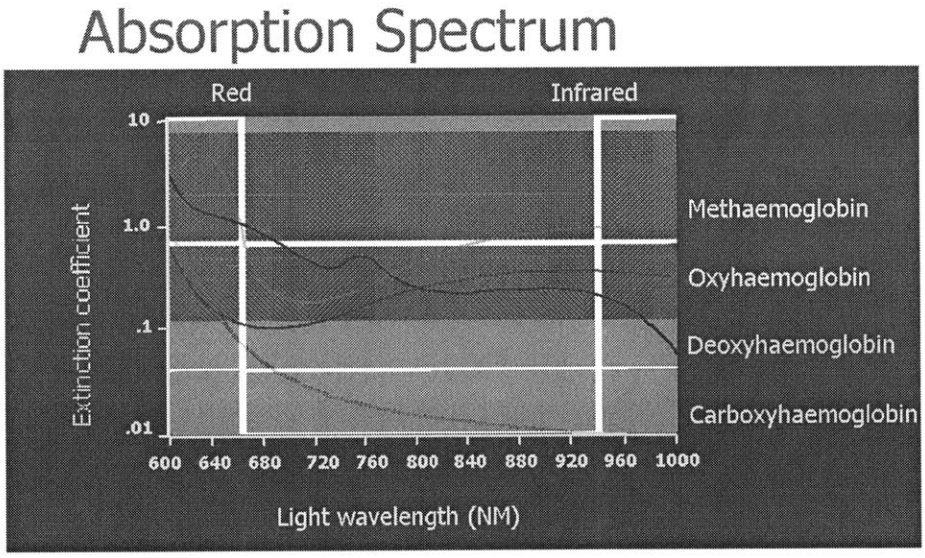

Adapted from:

http://www.health.adelaide.edu.au/paed-anaes/talks/brazil/oxygen/index_files/frame.htm

Figure 2.3 Absorption Spectrum

Focusing on the absorption spectrum for oxyhaemoglobin (HbO_2) and deoxyhaemoglobin(Hb) the different extinction coefficients can be found.

Table 2.1: Extinction Coefficients for Hemoglobin [4]

Wavelength [nm]	Extinction coefficient [L $mmol^{-1}cm^{-1}$]	
	Hb	HbO_2
660	0.81	0.08
940	0.18	0.29

The DC component of the signal is primarily affected by the absorption in the intensity of light source, ambient light, sensitivity of the detector, tissue bed, bone, venous blood, capillary blood, and non-pulsatile arterial blood [27]. The AC component captures the pulsating arterial blood (see Figure 2.4).

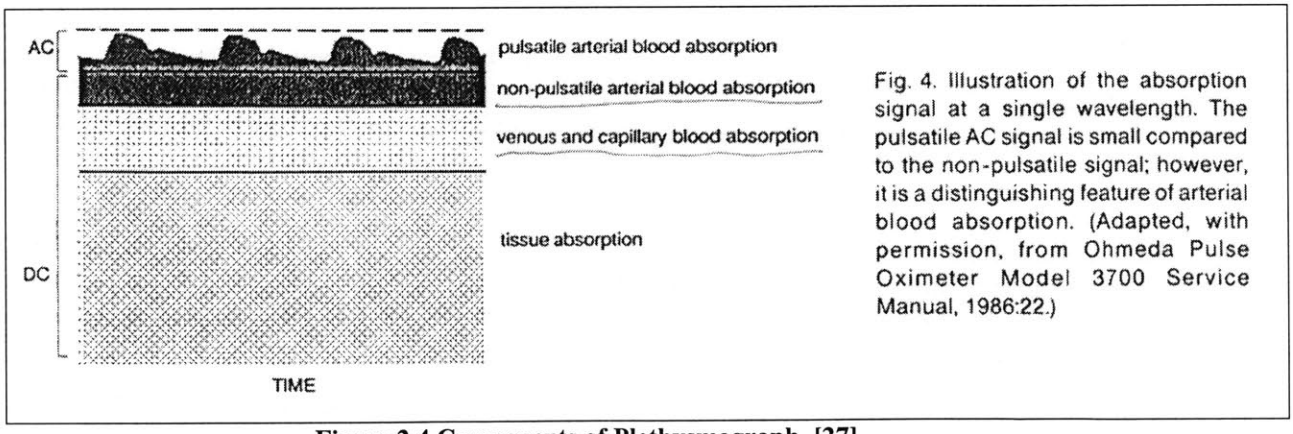

Figure 2.4 Components of Plethysmograph [27]

If the DC and AC component are known at two different wavelengths of light, then R can be computed, where R is given by the following equation:

$$R = \frac{AC_{660} / DC_{660}}{AC_{940} / DC_{940}} \qquad (2.2) \quad [24]$$

It has been proven that this ratio is empirically related to oxygen saturation (Figure 2.5).

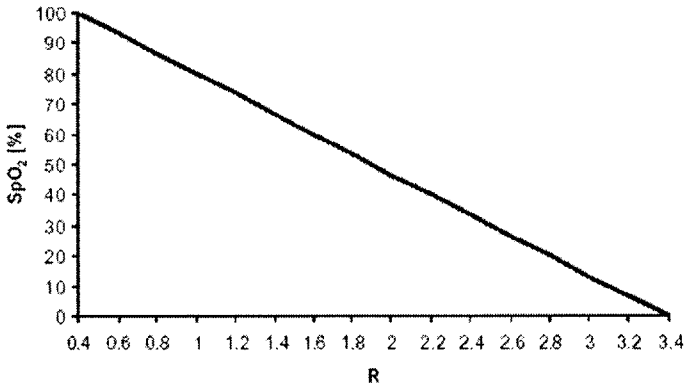

Figure 2.5 Pulse oximeter calibration curve. [24]

Therefore, possessing two LED wavelengths, one at 660 nm and one at 940 nm, the blood oxygen saturation level can be computed. In order to find the pulse rate, one of the two waveforms generated by the two different LEDs can be examined. With knowledge of the waveform, the beats per minute can be calculated, yielding the pulse rate.

2.3 Review of the Dynamics of the Arterial Wall

The previous ring sensor uses an elastic band to secure the optical components to the skin. It is held in place by applying a sufficient amount of a uniformed external pressure around the finger, but avoids causing discomfort to the wearer. The dynamics of the arterial wall will be analyzed to determine the sufficient amount of pressure. It is known that as the blood travels throughout the body through a series of capillaries, veins, and arteries. Each vessel has certain pressure but differs depending on the location of the body [8]. The arm has a blood pressure or 120 mmHg, while the finger has a blood pressure of 100 mmHg. These pressures can vary depending on the orientation of the feature. If the hand is raised or lowered, the internal blood pressure will be affected. This pressure, called the internal pressure, provides information regarding the health status of a patient. Knowledge of the internal blood pressure and the external blood pressure can yield the transmural blood pressure, given by the difference between the internal pressure P_i and external pressure P_o [19]. Knowing the transmural pressure, the radius of the artery can be computed. Therefore, if there is a small amount of external pressure applied to the finger, it produces a relatively small change in the radius of the artery, as shown in Figure 2.6. If the external pressure is further increased such that the transmural pressure approaches zero, the radius is the unstressed radius, which is shown by equation 4.3. In addition, a small change in the transmural pressure around zero, yields a large change in radius of the artery. This is due to the non-linear behavior of the arterial wall compliance, i.e. the slope of the radius-trnasmural pressure curve in Figure

2.6. Note that the compliance becomes maximized near the zero tranmural pressure. Assuming that the length of the artery is fixed, the volume of the blood in the artery is proportional to the square of the radius. Thus, as a result of the radius increasing, the

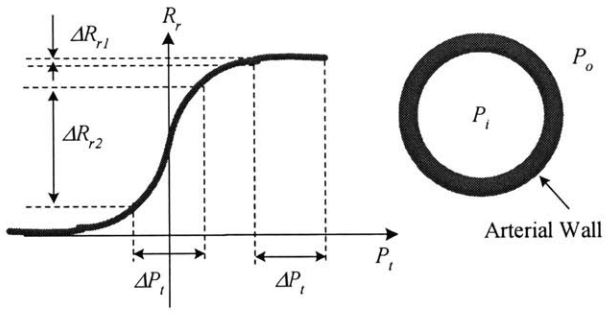

Figure 2.6 Change of arterial wall radius (Rr) with transmural pressure (Pt) [19]

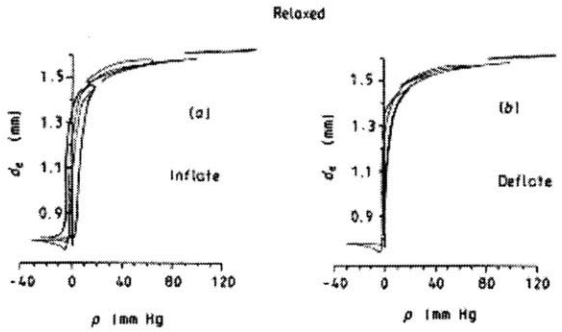

Figure 2.7 Pressure-diameter relationship of human digital artery. The pressure in the x-axis is transmural pressure ($P_i - P_o$), and the y-axis is external diameter. The external diameter is about 0.8 mm at when it is completely collapsed, implying that the wall thickness at the collapse is about 0.4 mm. [19]

blood volume increases, which causes the volumetric arterial pulsations to increase. If the external pressure is further increased, the transmural pressure decreases, which causes the artery to occlude. If an external force is further applied, complete occlusion develops.

$$P_t = P_i - P_o$$
$$P_i : blood\ \ pressure\ inside\ artery \qquad (4.1)$$
$$P_0 : pressure\ outside\ of\ \ artery$$

$$r[x] = r_0\left[1 - \frac{r_0}{Eh} p_t(x)\right]^{-1} \qquad (4.2)$$

Thus, sensor band applies enough pressure such that the occlusion does not develop in the artery, but supplies enough pressure to improve the signal.

2.4 ISSUES WITH THE PRESENT RING SENSOR

Although the previous design of the ring sensor has been proven to have comparable results to that of other pulse oximeters devices, there are some issues that remain. These issues include:

- Pinching effects
- Management of Wires
- Necrosis of the finger
- Motion Artifact
- Ambient Light

These drawbacks are addressed in this section. Based on the following, a new ring sensor will be designed to remedy these issues.

The previous ring sensor uses the notion of the inner and outer ring [19]. The outer ring consists of two sections: one that fits around the top of the finger base, and the

other section affix underneath the finger base. When these sections are brought together to secure onto the finger, they have the potential to possess a fraction of the skin in between its sections. When clamped together, a section of skin between the two sections is caught and squeezed causing the finger to feel a pinching effect. This pinch causes discomfort and pain for a short period of time.

The ring sensor possesses five 36 gage flexible wires used to connect the sensor band to the signal-processing unit. Though these wires are small, they are not robust when there is a small amount of interference. Also, if the sensor band is separated from the ring sensor unit beyond a certain distance, these wires detach themselves from the unit or from the sensor band. When this results, the LEDs do not get power nor the information from the photodetector is received. In either case, the output from the device is inaccurate. A method needs to be developed to reduce the occurrence of this problem.

The elastic sensor band provides a uniform pressure onto the skin to occlude the vein, but not interfere with the arterial pulsations. This was designed because the venous contribution is more susceptible to motion artifact. Therefore, occluding the vein results in a reduction of motion artifact sensed by the ring sensor. Though this uniform pressure can improve the signal, it also has the potential to cause discomfort for some users. If the finger is too large, occlusion will develop thus leading to necrosis if the band is applied for a long period of time. Necrosis is the pathologic death of one or more cells due to externally imposed forces [23]. Though the elastic band can be substituted for a different size band, the pressure exerted onto the finger cannot be adjusted. Thus, substitution of the elastic band is still problematic and time consuming.

In addition to the above problems, the previous ring sensor is continuously subjected to noise, but motion artifact is by far the main contributor [12]. Despite different means to reduce it, motion artifact still remains a constant issue for inventors, medical professionals, and patients. This motion causes the relative displacement between the skin and the photodetector to vary, as well as rotational effects placed on the ring sensor. It also affects the tissue mechanics of the body. A continuous change in the position of the finger has an effect of continuously changing the amount of light absorption from the tissue. Therefore, the amount of light contacted by the photodetector is affected. These factors make it difficult to obtain an estimate of the blood volume by photo plethysmography. The waveform is distorted resulting in inaccurate measured parameters. In addition, the analyst must locate all regions of motion to ensure that these regions be discarded when evaluating a patient. To provide a device for reducing motion artifact without causing ischemia, detecting motion, and notifying the analyst where the regions of motions are located will be beneficial.

The ring sensor utilizes photo plethysmography to obtain the pulse of the patient. Using this method requires use of a controlled light source and a photodiode. Though the band around the figure is elastic to ensure a tight pressure fit, the geometric shape of the board of the photodiode prohibits a fit free of gaps. Thus, an excessive amount of light due to an external light source, such as sunlight, can be detected by the photodiode. The increase in light causes the current of the photodiode to increase. If the current goes beyond a threshold, the first stage amplifier is saturated. This saturated pulse will not reveal the find the maximum amplitude of the signal nor the local extrema of the signal,

which can will lead us not being able to find heart rate variability, pulse, etc. To observe these saturations effects, this in depth, a model has been constructed.

The model is given by:

$$d = D\sin(\omega_d t) + d_0 \qquad Equation(6.1)$$

$$x = bA\sin(\omega\ t) + d \qquad Equation(6.2)$$

$$y = k\ sat\left(\frac{x}{a}\right) \qquad Equation(6.3)$$

,where d_o is the sunlight intensity, ω_d is the room light freq, D is the room light intensity, ω is the frequency of the pulse, A is the amplitude of the pulse, b is the LED intensity, a is the photodiode range, and k is the photodiode gain. Figure 2.8 is an example of the simulated model, assuming there are no ambient light effects interfering with the signal. Figure 2.9 shows the effects of increasing the ambient light. When this parameter is increased, the output is saturated at the crest.

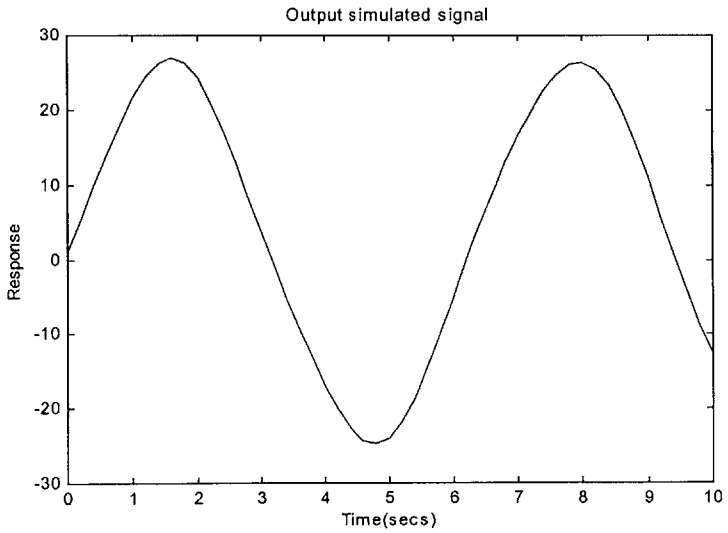

Figure 2.8 Modeled sinusoidal output signal

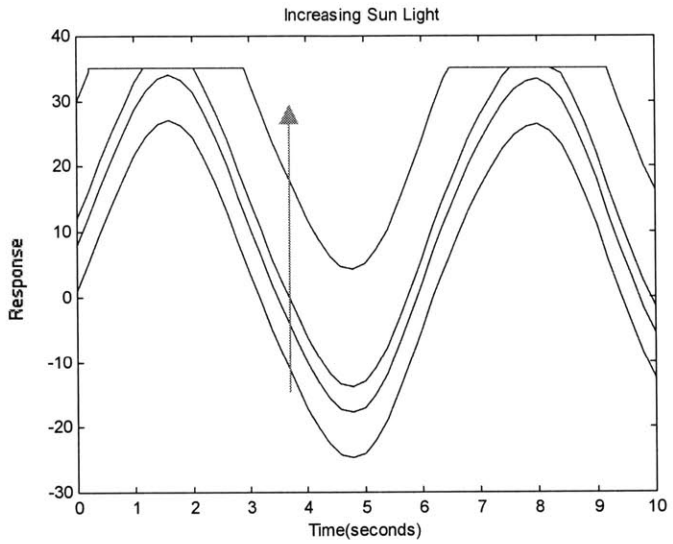

Figure 2.9 Model of the saturation effects due to ambient light

Note: this model assumes that the signal is a sinusoidal signal. This is sufficient since the signal received from a photo plethysmographic device is similar to a sinusoidal signal.

This section provided some insight to the issues, which plague the ring sensor. A new ring sensor was. In subsequent chapters, a new ring design will be presented to address majority of these issues. If issues are not resolved by hardware, additional signal processing techniques will be utilized to solve the remainder of these problems.

CHAPTER 3
DESIGN OF NEW RING SENSOR

3.1 New Components of the Ring Sensor

This new design consists of a housing unit, which will aid photo plethysmographic ring sensors. This device has been designed to remedy the issues discussed in the previous chapter. In addition, there were several design criterions established. First, the device must be lightweight such that the user suffers no long-term discomfort. Secondly, the device must be relatively easy to apply and disengage from the user. This process must have a relatively quick learning response and must have a change over time no longer than 2 seconds. Third, the housing unit must protect the optical sensors from outside interference other than ambient light. These interferences are due to a direct force applied to the sensory unit. Lastly, the device must have the capability to adjust the amount of pressure applied to the skin, in addition to providing a mechanism to ensure contact between the photodetector and the finger.

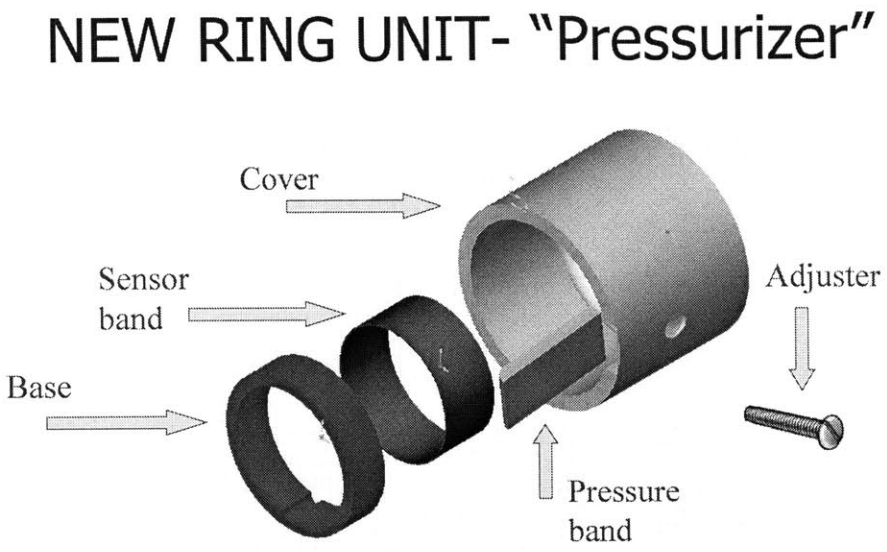

Figure 3.1 Components of Pressurizer

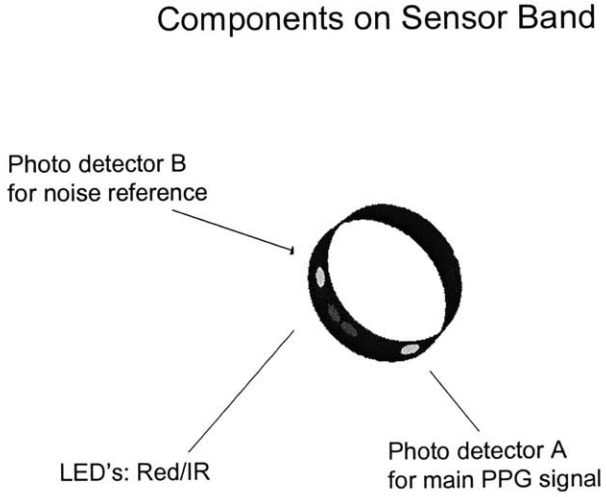

Figure 3.2 Components on Sensor Band

To address these various issues, the new ring sensor design termed, "The Pressurizer" arose. The Pressurizer consist of 5 major parts:

The Cover
The lightweight cover is made of a material made from cast acrylic. This unit has an inner diameter of 0.78 inch, but widens to 1.03 in diameter in order to interact with the base unit. The main function of the cover is to protect the sensors from outside elements. Also, it reduces the influence of external forces. Being decoupled from the sensor band, a direct force on the surroundings of the sensors will not affect the output of the signal. In addition, the cover unit serves in limiting saturation stemming from ambient light.

Base Unit
The base unit is made of the same cast acrylic material. With a tight tolerance of 0.01 of an inch diameter smaller than the inner diameter of the cover, this unit can connect with the cover to provide a secure fit by means of friction. The base units main function is to limit the elastic sensor band to only rotational motion. This component also manages small wires stemming from the signal-processing unit to various sensors located on the sensor unit. Moreover, this component aids in shielding the ambient light, which the cover unit could not handle.

Sensor Band
A tight elastic band used in the previous design of the ring sensor is replaced by an adjustable band. Because this band is made adjustable, it adds the feature of being flexible for fingers of various sizes. Having the sensor loose around the finger base

lowers the occurrence of necrosis. Like the previous sensor band, it possesses the photodetector and the two LED, which provides the photo plethysmographic response.

Adjuster

Because the sensor band is loose, the optical components are not secured around the finger base. The adjuster component provides contact between the photodetector and the skin. The adjuster places pressure directly on the finger base. In addition, the adjuster can tune the pressure applied such that the transmural pressure approaches zero to provide an improved signal. A setscrew is used for this application such that it is hidden from the view for aesthetic purposes.

Pressure Band

The pressure band is a rubber material whose main function is to alleviate direct stress on the photodetector. Without the pressure band, applying pressure directly on the photodetector can induce a sufficient amount of stress. If the stress is too intense, localized stress fractures can develop in the photodetector. This incidence will cause the photodetector to not operate properly. A pressure band relieves this induced stress. Also, using a pressure band applies pressure not only to the photodetector, but a small area around the photodetector. Therefore, the adjuster can be around a general area of the photodetector and still function properly.

Motion Detector

A second photo plethysmographic sensor is added to the sensor band to provide a means detecting motion. The sensor is located 90 degrees away from the location of the initial photodetector. By using the information of the provided by the 660 nm LED, venous

contribution can be measured. Because the vein is more susceptive to motion artifact, then this component will be able to detect motion. Since the band has been modified such that the vein is not occluded and the location of the sensor prohibits local occlusion, then a reliable detection system can be contrived.

3.2 On Board Signal-Processing

Previously, the ring sensor possessed a series of filters to reduce noise and recover the original signal. Though the ring sensor is capable of accomplishing this task, when transferred to the computer, noise can also result. This is especially true in a wireless network. In order to provide the original signal, additional processing was done on the signal.

Using a 4^{th} order Buttersworth Filter with a cut off frequency of 10 Hz, in to remove high frequency noise which might have appeared when taking the signal from the analog to digital converter, it is ensured that the signal is filtered. To ensure that drift or other factors causing the DC value to fluctuate, a high-pass 2^{nd} order Buttersworth Filter. This additional filter will eliminate the DC contribution, thus stabilizing the signal. This high pass filter is needed when using the detection method. Though pulsatile waveforms are evident, low frequencies cause them to be detected by a motion detection algorithm thus producing false alarms. Implementing this high-pass filter diminishes the occurrences of false alarms. This will be discussed in chapter 5.

3.3 Results

Using this new design alleviated the pinching effect with the current sensor unit. The new design is familiar to the user because it slides onto the finger similar to a finger ring. If the finger changes in diameter over time, two issues result: insecure attachment of the cover and base unit and discomfort. To alleviate this concern, the wearer has the option of resizing the unit or exchanging the size of the unit. This process is familiar to those accustomed to finger rings and only happens over a significant duration in time.

Grouping all wires together with a heat shrink wires enables the five wires to be condense into one. Allowing the wires to be routed through the base unit allows a relief on stress onto the system. These wires are lead into to a flex connector, which is attached to the signal-processing board. If the flex connector is interfered with by a disturbance, it is durable enough not to break connection with the signal-processing unit or the detectors themselves.

Implementing an adjustable band remedies the potential issues of necrosis. If the finger varies in size or discomfort is felt, the band can be adjusted to accommodate the user. Since there is relatively no pressure exerted onto the skin, ischemia will be avoided. Using the adjuster to pressurize a small area of the finger base, the signal can improve the quality of the signal with out impeding the blood flow. This will be the center of discussion in chapter 4.

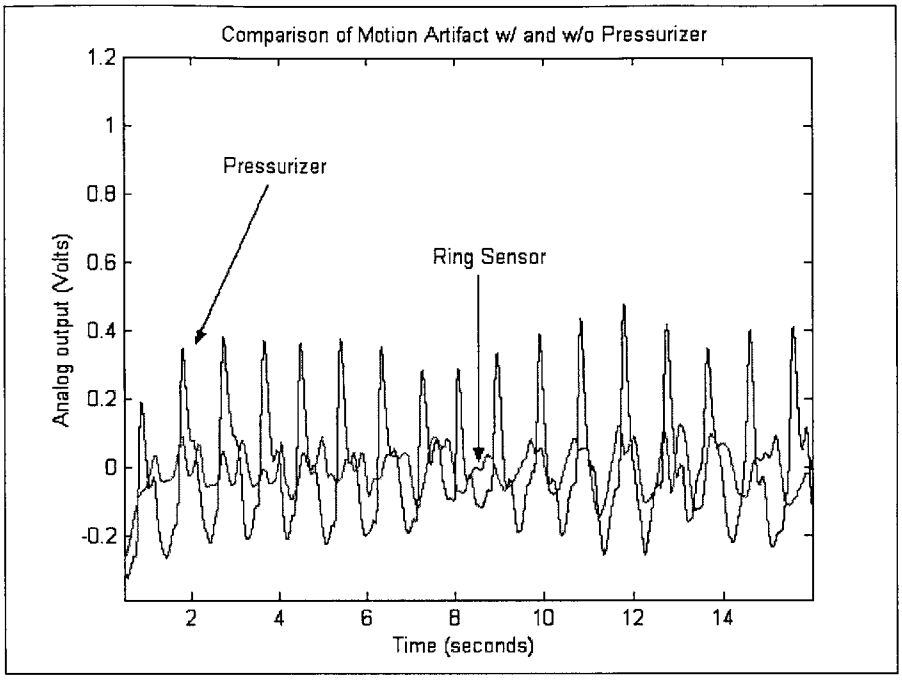

Figure 3.3 Performance of new design under motion

Because the band is loose, a small disturbance can cause the displacement between the skin and the sensor to vary. Using the adjuster to ensure that the photodetector is secure to the skin, a small disturbance causes no displacement between the detector and the skin. Therefore, the analog output is not disturbed and thus a reliable measurement can be made. In figure 3.3, a hand is moved back and forth at a frequency less than 1 Hz. The band in both the Pressurizer and the ring sensor were loose to avoid ischemia. When analyzing the graph, the Pressurizer performs better the ring sensor, thus reducing motion influence. Motion detection will be discussed in chapter 5.

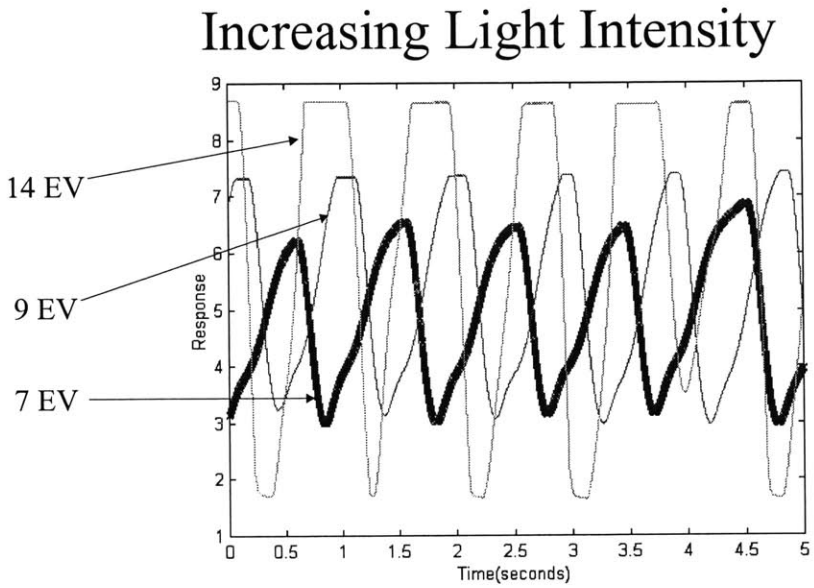

Figure 3.4 Experimental effects on increasing ambient light intensity

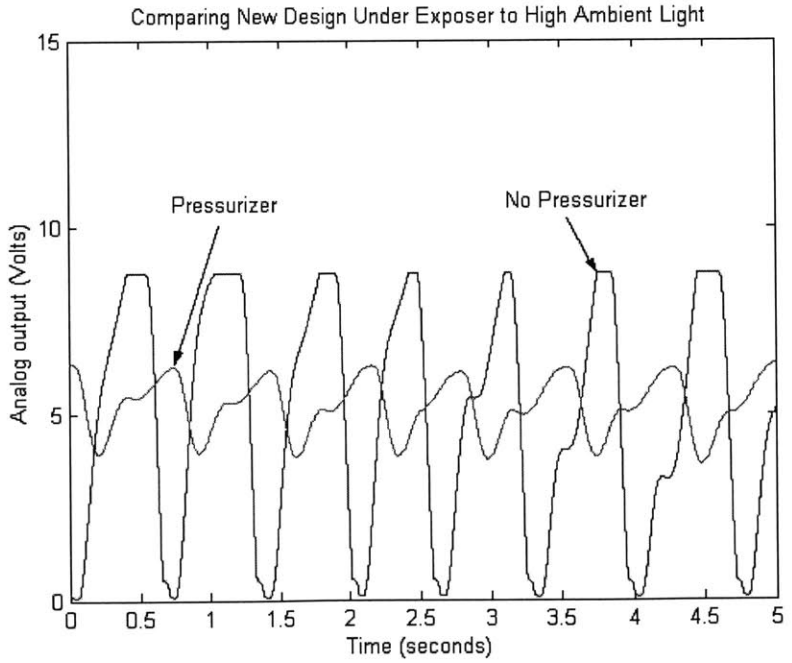

Figure 3.5 Pressurizer's response of ambient light (intensity of 12 EV)

Ambient light has the ability to saturate the operational amplifiers in the signal-processing unit. Figure 3.4 shows the effects of ambient light on photo plethysmographic devices when increasing the ambient light. As the intensity of light increases, saturation becomes more evident. This experimental data agrees with the model developed in chapter 2. Although techniques such as using a logarithmic amplifier or diodes to avoid saturation, another solution can be found by hardware solution. As stated in previous sections, the cover and the base unit of the Pressurizer shield ambient light from the sensors. Figure 3.5 shows that the Pressurizer does improve the sensor quality.

In addition to reducing the issues presented, various constraints such as size, weight and power consumption where checked to see if they were comparable to the previous ring design. The weight of the outer ring was compared to the weight of the cover and base of the new prototype ring sensor. Only these components were compared since the other components remain unchanged or were negligible compared to the housing unit. The outer ring from the original ring sensor weighed 6.81 grams. The Pressurizer's cover and base unit weighed 9.05 grams. This difference in weight equated to the weight of a dime. Therefore, the unit has met weight constraints. The design did not change the signal-processing unit nor added any additional power. Therefore, the original constraints of the ring sensor were met.

The upcoming chapters will focus on two key issues: motion detection and the improvement of the signal while avoiding the possibility of necrosis.

CHAPTER 4
EFFECTS OF PRESSURE

4.1 INTRODUCTION

This section focuses on how to improve the ring sensor by increasing the signal-to-noise ratio (SNR), without reducing circulation interference. In the processing unit of the ring sensor, the signal passes through a series of gains to amplify the signal. The end result consists of a pulse waveform with relatively low amplitude. Considering the magnitude is on the order of microvolts, it will be advantageous to increase the signal in a manner such that the SNR will be improved.

As stated in the background section, the SNR can be improved by exploiting the non-linear behavior of the arterial wall compliance (see Chapter 2). Therefore, applying an external force such that the transmural pressure will approach zero the pulsations will increase in magnitude. Thus, the SNR can be improved. .

Low pulse amplitude

Some patients have low pulse amplitudes making the pulse detection difficult on current blood monitoring devices. When patients are exposed to environmental changes, such as temperature, the amplitude of the waveform is affected. When the ambient temperature falls, the body begins to have a reduction in heat. Though the body tries to accommodate this heat loss by shivering (an attempt to warm the body by the involuntary

contraction of skeletal muscles), the hypothalamus responds by generating a cutaneous vasoconstriction. The hypothalamus is the part of the brain that lies below the thalamus, forming the major portion of the ventral region of the diencephalon and functioning to regulate bodily temperature, certain metabolic processes, and other autonomic activities. During this vasoconstriction stage, restriction of blood flow is caused when there is a decrease in arterial pressure. When this results, the barorecepetors in the body decreases in firing, thus causing the sympathetic discharge to increase in firing. This results in vasoconstriction [11]. Since the body attempts to preserve blood for the legs, heart, and brain, the extremities are the first to feel the affects of vasoconstriction due to temperature. In addition, 90% of the functionality of the finger is used for thermoregulation [26]. Thus in cold environments, the finger is very susceptible to temperature. The new ring design has the ability to apply local pressure to ensure the contact between the skin and the photodetector. Applying further external pressure will increase the pulse waveform amplitude. Therefore, the new ring sensor will improve the SNR.

Circulation Interference

The heart pumps blood continuously, circulating oxygen and nutrients throughout the body. When using a traditional cuff or any device that applies a uniform surface pressure onto the finger or the arm, it constricts the blood vessel, thus limiting or impeding the amount of blood supplied to the areas. These actions result in a lack of nutrients and oxygen to these areas causing ischemia. Though these actions are feasible for short-term use, they cannot be applied for a significant duration of time. If

constriction persists for long period of time, necrosis will result. Thus, the wearer cannot be exposed to these devices that use these measurements long-term. For an anemic patient, cutting off the blood supply will cause serious injury, including death.

In addition to improving the SNR, the new ring sensor design will show circulation is not affected throughout the finger. To observe these characteristics, two different methods are presented: uniform pressure and localized pressure. To observe the improvements in SNR, the pulse waveform was observed by the ring sensor at the finger base. If there was a significant increase in amplitude, then the SNR was improved. An additional device, a FDA-approved photo plethysmograph sensor produced by Nellcor was applied at the fingertip. This device was used to measure amount of circulation interference. To observe the effects of interference, various types of pressure were applied to the individual. If the fingertip showed no effect regardless of the effects at the finger base, then there was circulation interference.

To observe the occurrence of circulation interference, a uniform pressure by means of a finger cuff was applied to the base of the finger. The pressure was increased until occlusion resulted. It will be shown that these methods improve the SNR, but potentially constrict blood flow. To observe the effects of localized pressure, the new ring sensor design was applied. The pressure was increased until the amplitude reduced to a certain point. Complete occlusion never resulted. Thus, it will be shown that this method increased SNR while not restricting blood flow throughout the finger.

4.2 Effects of Uniform Pressure

Calibration

To improve the signal-to-noise ratio, a uniform pressure can be applied to the surface of the skin. In this section, the base of the finger was pressurized.

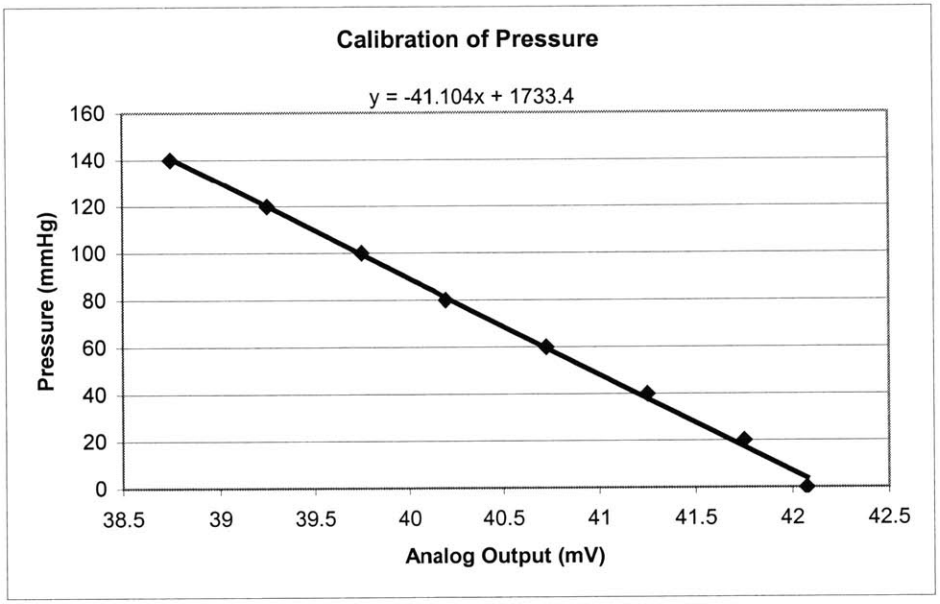

Figure 4.1 Calibration of pressure

Using a blood pressure transducer the blood pressure was converted from a pressure to an analog voltage. The PowerLab 410 interface captured this voltage. The blood pressure was increased from 0 mmHg to 140 mmHg in intervals of 20 mmHg. The data was recorded at every interval. Figure 4.1 shows linear relationship between the analog output of the blood pressure transducer and the blood pressure. Therefore, the transducer was calibrated.

Set-up

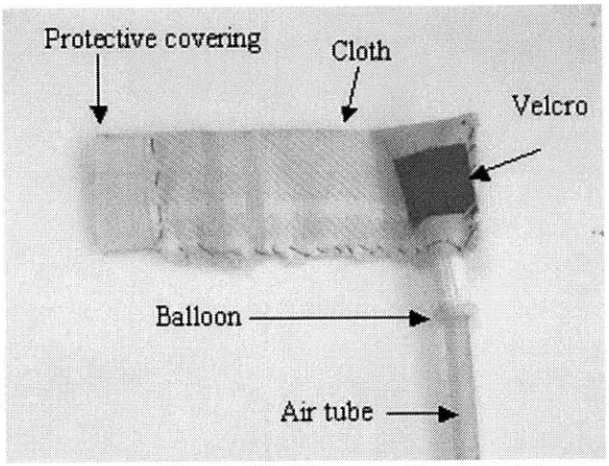

Figure 4.2a Finger cuff apparatus

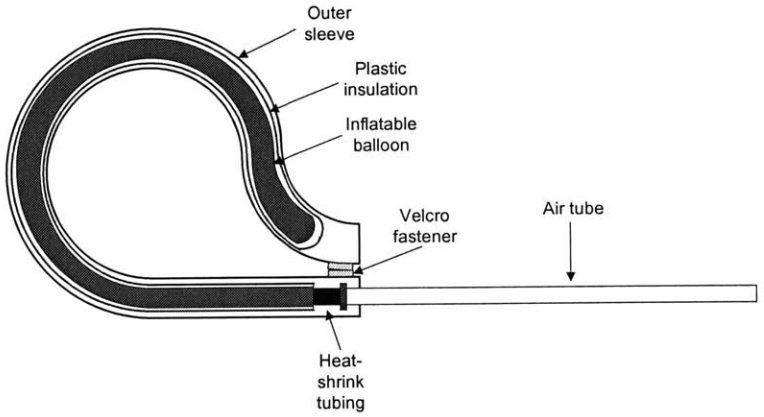

Figure 4.2b Finger cuff apparatus (schematic)

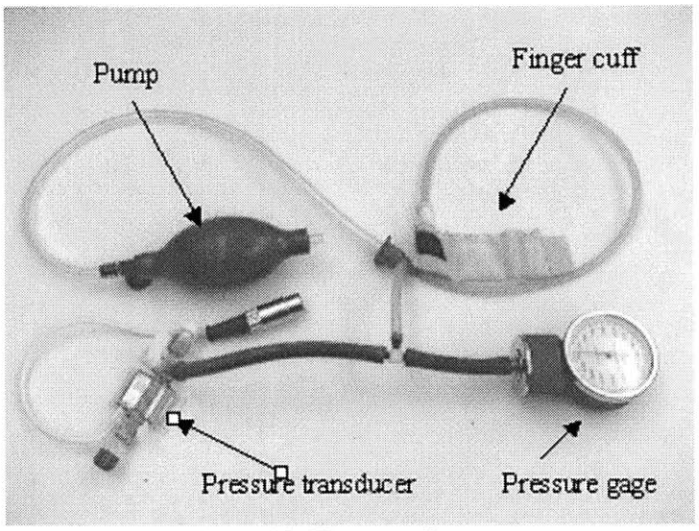

Figure 4.3 Finger cuff set-up

To further investigate the effects of uniform pressure along the finger base, a finger cuff was constructed using cloth, balloon, shrink wire, thread and a needle (Figure 4.2). Using this apparatus in addition to a pressure gage, pressure transducer, and a pressure controller, pulse amplification and blood circulation were examined. The pressure gage was to verify the pressure applied (Figure 4.3).

Pulse amplification

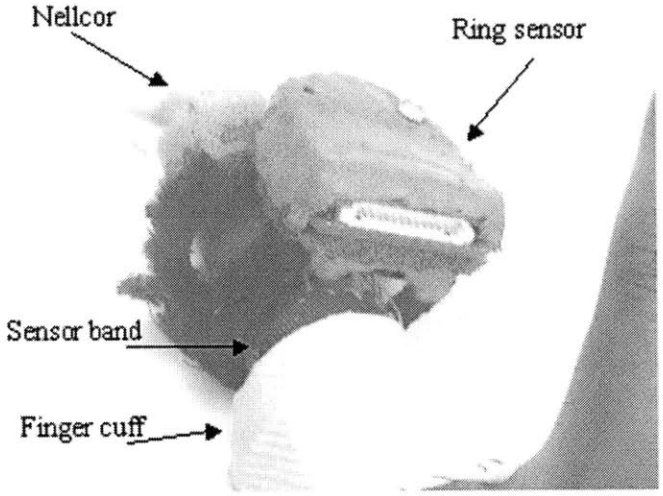

Figure 4.4 Experimental setup of finger cuff

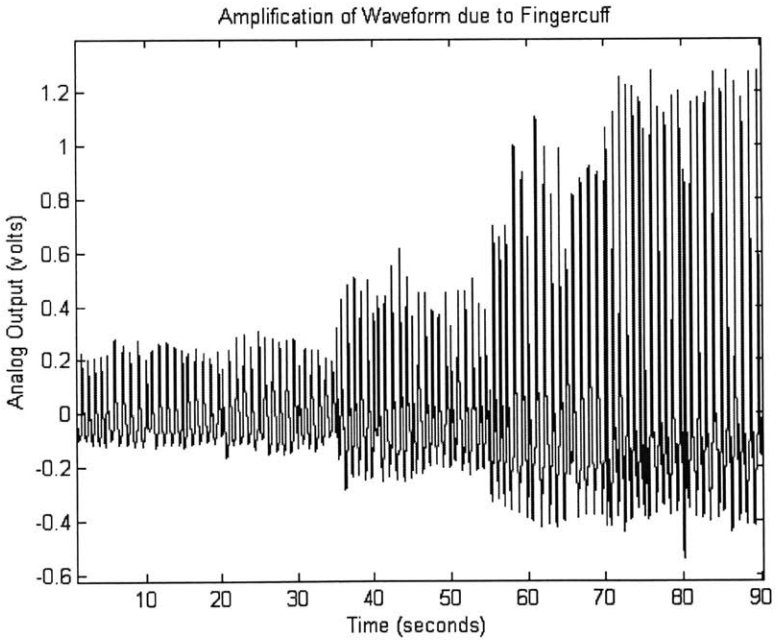

Figure 4.5 Pulse amplification due to finger cuff

The ring sensor was applied to the finger base. The finger cuff was placed between the ring sensor band and the knuckle (see Figure 4.4). To increase the amplitude

of pulsation, a finger cuff was applied to the finger. Using only the sensor band and signal processing unit, the photo plethysmograph waveform response was generated. This is shown in Figure 4.5.

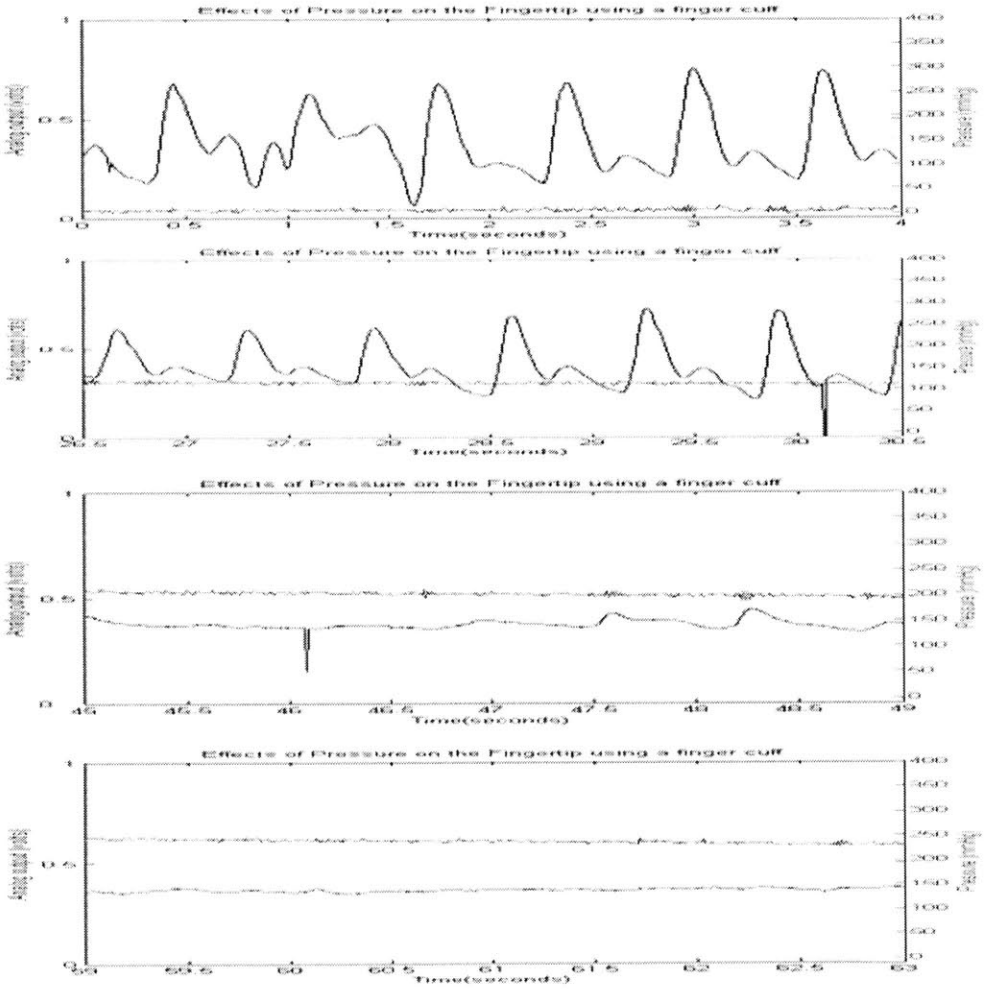

Figure 4.6 Comparison of pressure and amplification at the fingertip using finger cuff

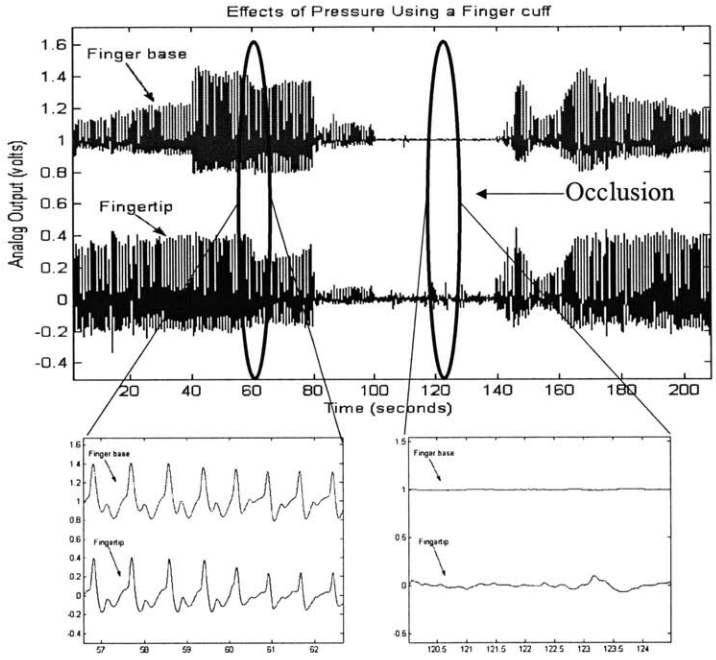

Figure 4.7 Effects of occlusion by application of finger cuff

To measure the amount of interference, a Nellcor sensor was placed at the fingertip. When pressure was exerted onto the finger base, there was a point where arterial pulsations ceased at both the finger base and the fingertip. Thus, the vein and the artery were occluded. This provided a lack of nutrients to the finger. This is shown in Figure 4.6 and Figure 4.7. Figure 4.7 examines the relationship between pressure and the volumetric pulsation until occlusion. As the pressure is increased, occlusion resulted. As the pressure is lessened slowly, circulation resumed to the fingertip. When analyzing the Figure 4.8, the initial diagnostic might seem that the increasing pressure had no affect on the fingertip, thus showing there was no interference when using a cuff. This was due to the fact that the finger consists of a network of veins and arteries. When the blood was

restricted locally, the body reacted by pumping enough blood such that a sufficient amount of blood was supplied to the fingertip. Since the finger base was the location where the pressure was applied, the ring sensor was affected. At a specific pressure, the pressure was far to great to be compensated by the body and in turn affected the fingertip. As the pressure increases, the blood vessel became further condensed, thus restricting blood to all essential areas of the finger. Again, when this pressure was exerted for a short period of time first, discomfort was felt on the finger. A tingling feeling developed on the finger since there was no blood supplied. This feeling diminished when the pressure was lessened.

4.3 EFFECTS OF A LOCALIZED PRESSURE

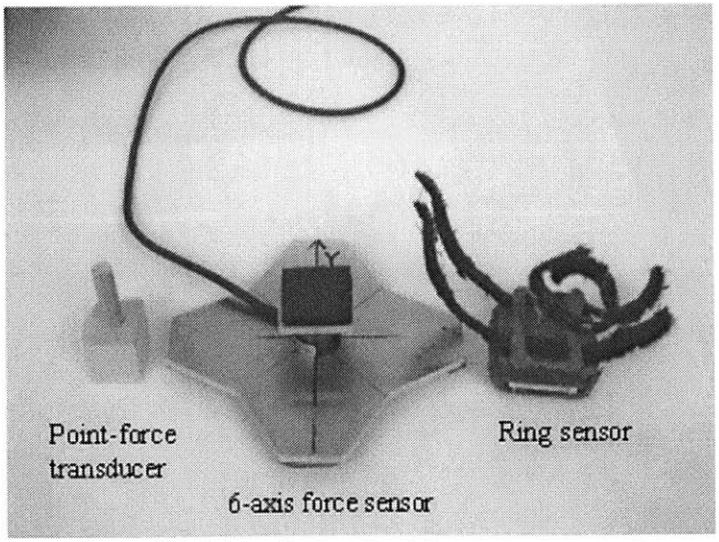

Figure 4.8 Set-up for localized force measurements

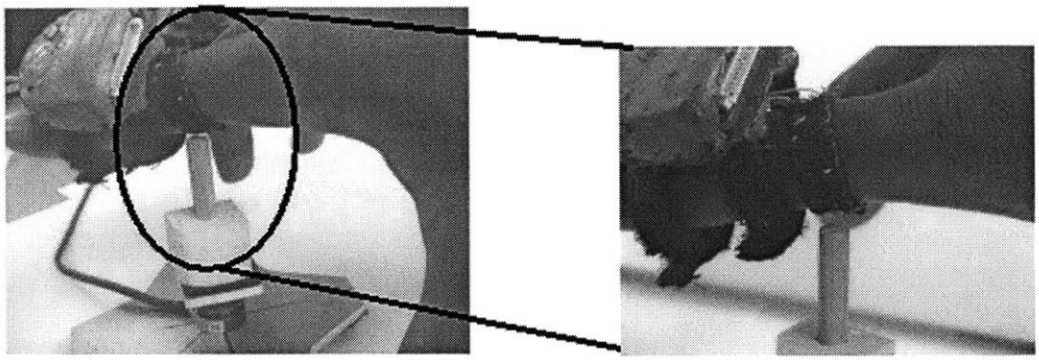

Figure 4.9 Application of set-up for a localized force measurements

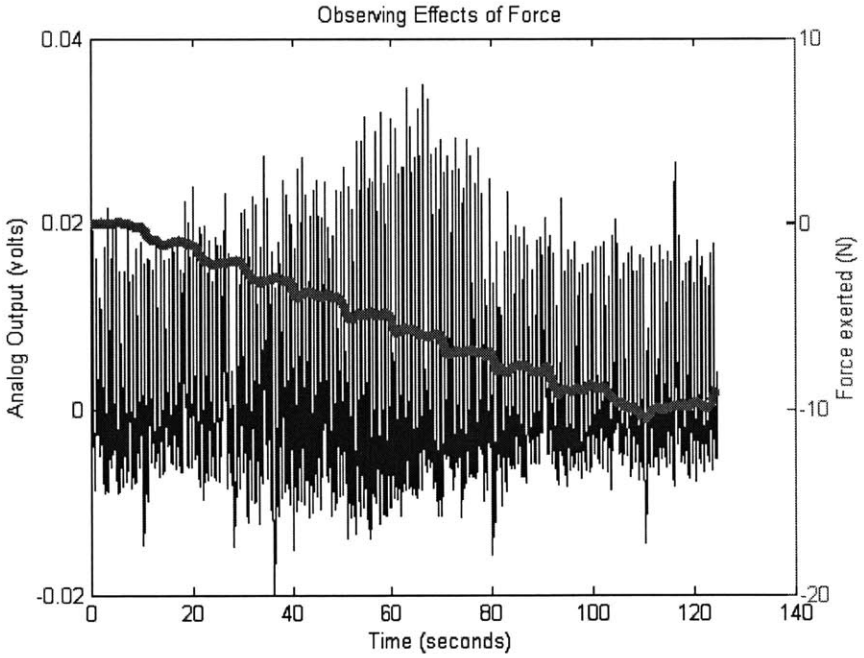

Figure 4.10 Observing the effects of force exerted locally at the finger base

A force-point transducer, ring sensor, and a six-axis force sensor were used to observe the behavior of the photo plethysmographic response due to changes in localized force. Figure 4.8 shows these components. The force was found by pushing the finger

downward direction onto the force-point transducer. The transducer had a circular contact area, which had a diameter of 0.25 inches. The transducer was placed on top of the six-axis force sensor. This process is shown in Figure 4.9. The applied force on the finger base has a reactionary force at the force sensor. This enabled the measurement of the applied force. As the force increases, the photo plethysmograph amplitude increases, until it reaches a maximum as shown in Figure 4.10. This maximum point is the systolic pressure. As the force is further applied, the amplitude begins to decrease. Force and the photo plethysmographic waveform were taken simultaneously. To improve the signal-to-noise ratio, an alternative method using the new ring sensor design was investigated.

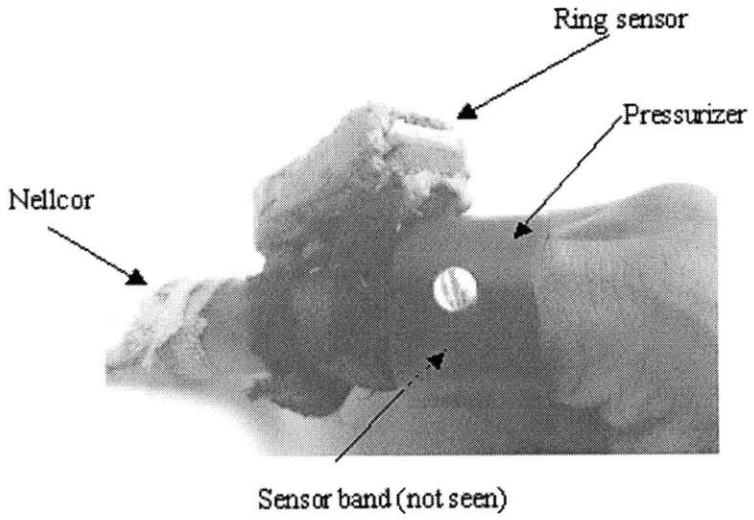

Figure 4.11 Prototype of the new ring sensor design

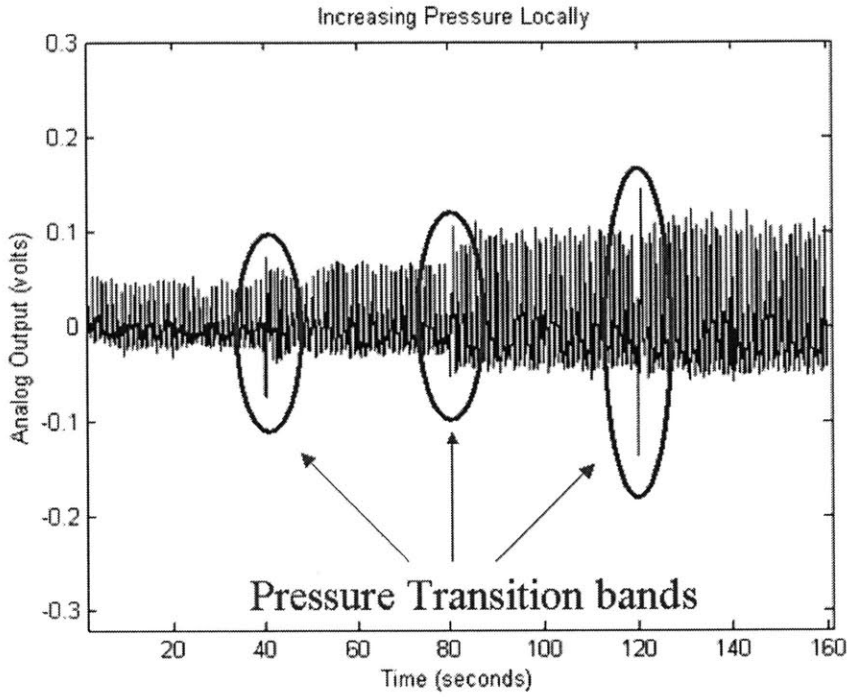

Figure 4.12 Applying a pressure locally to photo plethysmograph waveform

Pulse amplification

The new ring sensor was used to observe its effects on local pressure. Although pressure is applied only at a localized point, it is expected that the volumetric arterial pulsations increase in amplitude. Having a localized pressure also ensures contact between the elastic band and the skin as mentioned in chapter 3. The Pressurizer was adjusted to ensure contact, as well as to apply to small amounts of pressure on the tissue. Figure 4.11 shows the photo plethysmographic signals measured at three different pressures. As the pressure is increased, the waveform amplitude increases. The transition bands are regions where the pressure was increased. Therefore, the signal-to-noise ratio is increased.

Reduced Circulation Interference

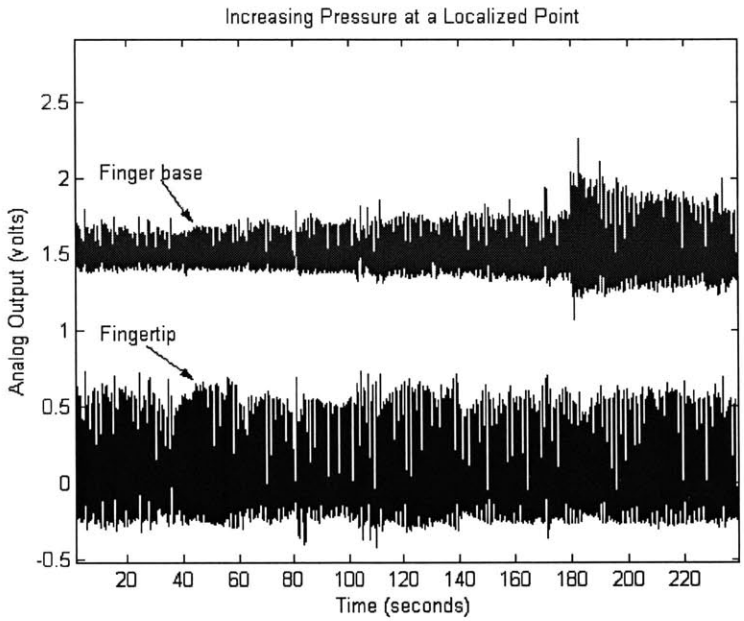

Figure 4.13 Observing the effects of local pressure at the fingertip and the finger base

To measure the interference effects when using the localized pressure enhancer, the ring sensor was applied at the base while the Nellcor was located at the fingertip. Placing the Pressurizer at the finger base, local pressure was applied, thus causing the waveform at the finger base to be influenced. Figure 4.13 shows the fingertip was unaffected although sufficient amounts of pressure were applied to the base of the finger. Since only a small section of the finger base was exposed to this force, only one of two digital arteries was affected. Knowing the fact that the finger consists of a network of veins and arteries, inducing a local pressure at the finger base, only constricted the vessel

locally. Blood flow is unimpeded along the second digital artery. Thus, nutrients and oxygen were supplied to the fingertip showing no signs of circulation interference

4.4 Comparison of Methods

The difference between the Pressurizer and traditional methods is the fact that the cuff is restricting all blood flow into the finger. When comparing the results from the pressurizing the finger at a local point or along the uniform surface, it is clearly seen that both methods amplified the waveform. Further increasing the pressure will yield the localize method to increase then decrease in volume, without impeding the blood flow to the fingertip. When increasing the pressure with a cuff, the amplitude will also increase then decrease. At a certain point the artery will be occluded thus proving no blood flow to the finger. This is due to the fact that the there is a network of veins and arteries in the finger. When pressurizing the finger locally, one digital artery is occluded, but there are other pathways which the blood can travel to reach essential areas of the finger. When using a cuff to pressurize the finger, no matter the number of different pathways the blood can travel, all pathways are blocked. Thus, it is shown that the new design gives the ring sensor an improvement on SNR without impeding blood flow. Likewise, it gives the ring sensor the added feature of adjusting external pressure, which increases the transmural pressure.

4.5 Observation of Occlusion at the Arm

Though it has been shown that localized pressure does not occlude blood flow, occlusion of the finger can result in other ways. For instance, if the arm is rested on object, gravity might apply enough pressure such that occlusion of the artery may occur. The blood flow is lessened creating a tingling feeling or numbness. During this process oxygen perfusion is disrupted causing tissues, muscles, and other essential anatomical elements to fail to receive nutrients. Because occlusion of the arm leads results in occlusion of the finger, it would be beneficial to have a device, which validates the signal, provide the location of occlusion, and alert the medical professional during occlusion. In this section, the behavior of arm occlusion will be observed in order to develop a method of to detect arm occlusion.

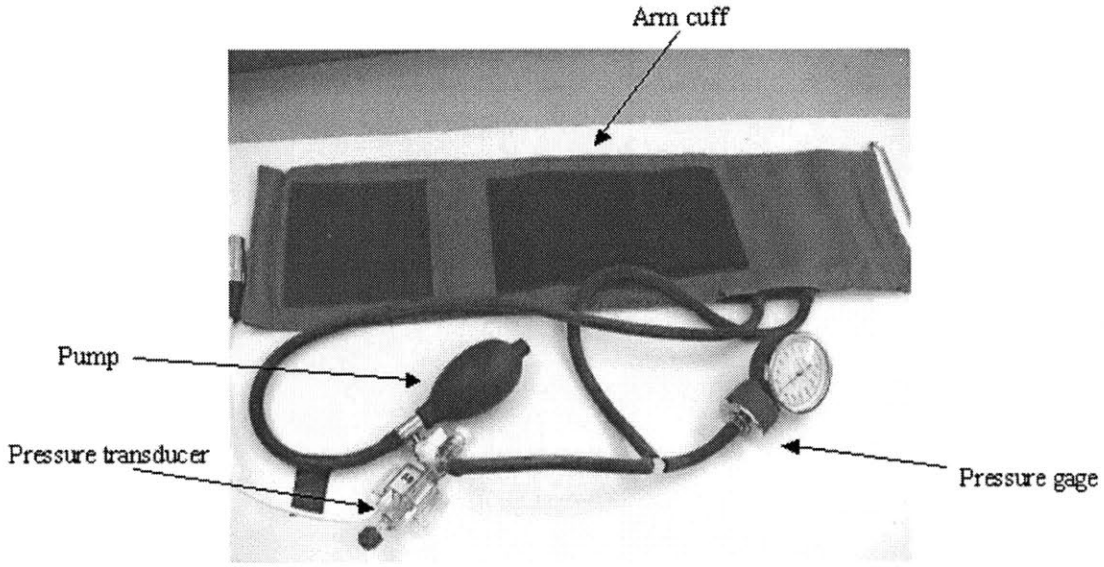

Figure 4.14 Arm cuff set-up

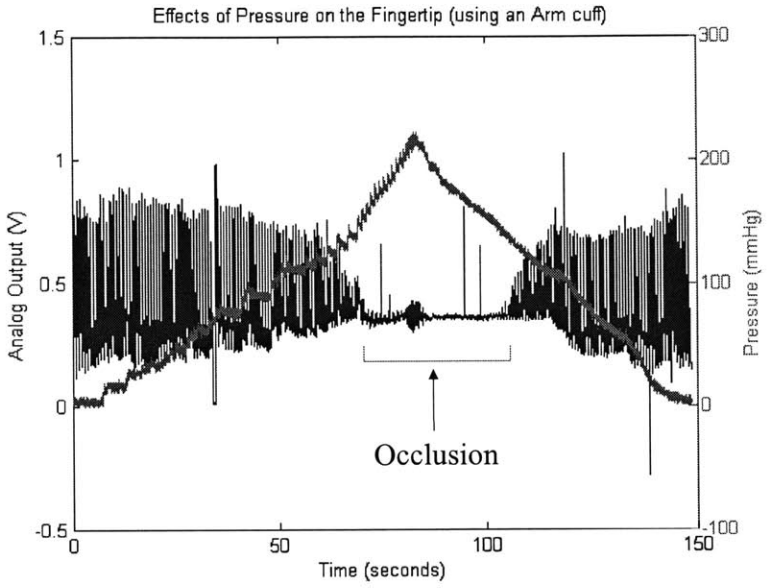

Figure 4.15 Effects of pressure at the fingertip using an arm cuff

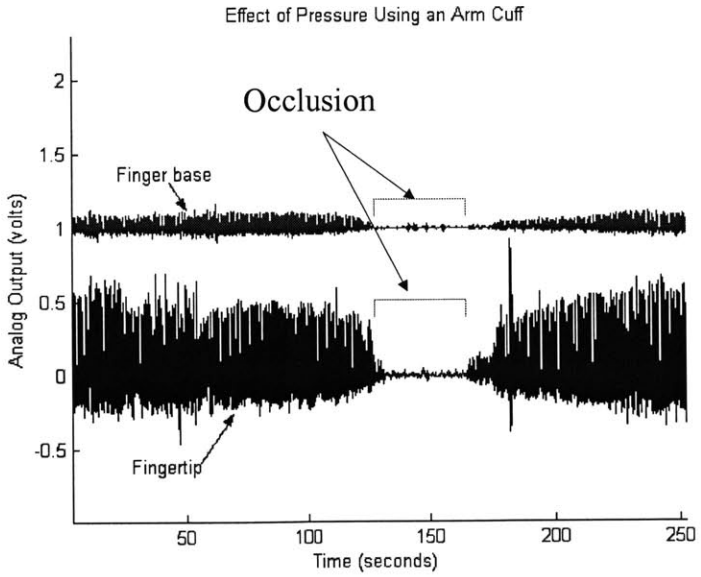

Figure 4.16 Effects of occlusion by application of an arm cuff

To observe the effects of the effects of arm occlusion, a traditional blood pressure cuff was applied to the arm of a health 26 year old. This uniform external pressure was steadily increased to observe the characteristics of the finger base and the fingertip. The waveform showed no significant effect until the pressure exceeded a threshold value. At this value, the cuff began to restrict blood flow along the arm and the finger. The amplitude of the volumetric pulsation of the artery was reduced as a result of this restriction. Further increasing the pressure, pulsations cease around 145 mmHg. This value marked where complete occlusion of the blood artery results. During occlusion, no blood was propagated throughout the finger, which resulted in a loss of oxygen and other nutrients to the finger. Figure 4.15 shows the relation of the photo plethysmographic response of the sensor measure at the fingertip and the pressure. Figure 4.16 shows how circulation was impeded at the finger base and the fingertip. When comparing these results to those of the finger cuff, it can be seen that the arm cuff occluded with a faster time constant that the finger cuff. Knowing the relative amplitude of the arterial volumetric pulsations at different time instances, a decision can be made on whether occlusion is developing at the finger base or the arm. More experimental results need to be performed to verify this result.

CHAPTER 5
MOTION DETECTION

5.1 INTRODUCTION

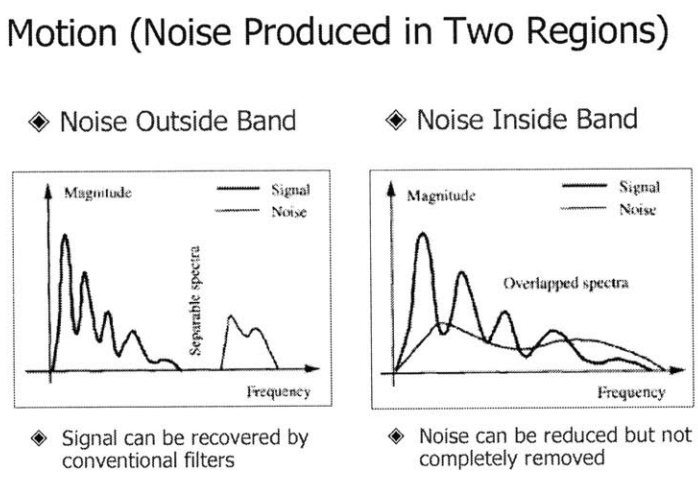

Figure 5.1 Motion influence on signal [25]

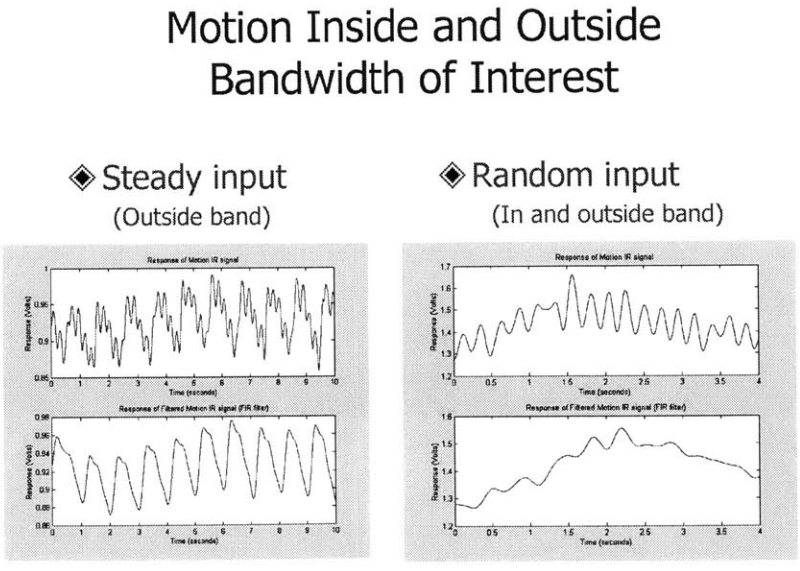

Figure 5.2 Effects of Motion Inside and Outside Bandwidth of Interest

One of the most common problems with photo plethysmographic sensors is due its use of optical sensors. These optical sensors are susceptive to motion artifacts. Motion artifact can exist due to "mechanical forces giving rise to changes in optical probe coupling, patient physiology, optical properties of tissue due to geometric realignment, or complex combinations of all these effects" [12]. Because these sensors are primarily used when the patient is physically immobile or required to be stationary for a period of time, they are continuously used in the medical arena. For patients who are demented, paralyzed, or unconscious, long-term monitoring can be done. For patients who do not possess these features, remaining still for an extended period of time is illogical. Thus, it is reasonable that motion artifact will be introduced into the system.

Motion artifacts introduced into the system consist of both low and high frequency disturbances. Classical filters can be applied to recover the pulse from a noisy signal, but in most cases the noise spectrum overlaps with the signal spectrum (Figure 5.1). Thus, it is extremely difficult to recover the signal, especially when there is a significant contribution of noise in the same bandwidth of the signal. Figure 5.2 illustrates this point. In the first instance, the figure shows the frequency of perturbation is outside the signal spectrum. Thus, classical filtering techniques will be sufficient to recover the signal. In this case a frequency of 5 Hz was applied to the system. Using a low pass FIR filter with a cutoff frequency of 3 Hz, the motion was filtered out and the original signal was recovered. In the second instance, a motion was generated by hand fluctuation to induce a random motion. Using the same FIR filter, the original signal could not be recovered.

Thus, having a detection system in place would help to determine if the pulse is recovered or if there still is a major contribution of noise. If there were means to detect whether the ring is influenced by motion, it would make the device more efficient. When developing a detection system for non-invasive biological measurement devices, the system provides an indicator to the user, informs an analyst the regions of detected motion, or causes the device to refrain from taking data until motion subsides. In addition, specifications for the ring sensor must be met. These specifications include: the size the ring sensor must remain intact, the overall power consumed must not increase significantly, and the computational time must be in a manner of seconds. The detection system must possess a small number of false alarms and miss detections. If the false alarms are abundant, it can lead to unnecessary panic and ultimately ineffective. If there are a sufficient amount of miss detections, the information obtained will be inaccurate. Both instances will lead to an unreliable unit and can lead to a decline in use. The previous ring sensor does not provide a method to detect motion. Thus, proving this added feature would prove to be beneficial.

In this chapter, four methods for motion detection will be considered: accelerometer, maximum likelihood method, autocorrelation technique, and an additional motion detector. After observing these various methods, a decision will be made. This decision will be based on its abilities to meet various constraints, and its overall performance.

5.2 Accelerometer

Accelerometer is to measure an inertial force when the sensor body is accelerated. If assuming the system only consists of a mass, spring, damper system, then the force can only come from the spring. Since the deflection of the spring, is proportional to force, which is proportional to acceleration, then the acceleration can be measured if the displacement is known [6]. Different accelerometers have different methods in the evaluation of this distance. Deflection type accelerometers use unbonded and bonded strain gages, piezoelectric materials, and angular methods to measure distance. Null-balance accelerometers use feedback to achieve more accuracy than that of deflection type accelerometers. Based on the output of the accelerometer, it can be determine if acceleration is present. If the accelerometer measures a sufficient amount of acceleration, then the ring sensor or display unit can decide if motion exists. Therefore, the accelerometer can be incorporate into the ring sensor and can decide if the wearer is mobile or stationary.

5.3 Maximum Likelihood Method

The maximum likelihood method is another way to detect motion artifact. Maximum likelihood approach classifies the measurement made. To use this approach, there are three measurements required: the number of events has to be known, each events probability density function, and prior knowledge on each event. Given a photo

plethysmographic signal, there are two events: 1) the signal does not contain motion artifact, 2) the signal does contain motion artifact. After establishing these two events, the probability density function (pdf) for both events has to be known. Assuming that there are a vast number of trials, the models will converge into a Gaussian pdf by the central limit theorem. Therefore, certain features must be obtained to develop the pdf. Their features include the mean and variance.

Knowing these parameters, the Gaussian pdf can be constructed.

$$f_X(x) = \frac{1}{\sqrt{2\pi\sigma^2}} e^{-\frac{1}{2}\frac{(x-\pi)^2}{\sigma^2}} \qquad (5.1)$$

When the pdf is known for the each corresponding event, then a decision criterion can be established. Below is the classification approach used.

$$\frac{f_{R|H}(r \mid H_1)}{f_{R|H}(r \mid H_0)} \underset{'H_0'}{\overset{'H_1'}{\gtrless}} \frac{p_o}{p_1} \qquad (5.2)$$

, where R is the random variable measured, H_0 and H_1 are the to possible models, p_0 is the prior probability of event H_0 happening, p_1 is the prior probability of event H_1 happening, and $f_{R|H}(r|H_o)$ and $f_{R|H}(r|H_1)$ represent the conditional densities on the distribution of a measured variable under the two events [15]. Assuming there is an equal probability for motion or no motion to be present in the signal, the decision rule can be reduce to

$$f_{R|H}(r \mid H_1) \underset{'H_0'}{\overset{'H_1'}{>}} f_{R|H}(r \mid H_0) \qquad (5.3)$$

In order to find the model of the pure signal and a motion-influenced signal, a pdf was contrived using the experimental data. The intensity value was used as the measured random variable. The intensity value was chosen because motion artifact causes the amplitude of the waveform to be significantly different than the arterial volumetric pulsations. Thus, this variable will be used to detect motion.

5.4 Autocorrelation Method

Another method available is the autocorrelation method. This method also can be used to determine if the signal captured is influence by motion. It is known that the pulse is a periodic signal. Though an individual's pulse might increase or decrease, depending other the nature of the activity or their present health status, the pulse change in frequency. Though the frequency can change, the pulse still remains a periodic signal. When random motion is introduced in the system, it is mainly non-periodic. Exploiting this fact, a distinction can be made between a motion signal and a purely biological signal.

Given a wide sense stationary signal, the autocorrelation function is defined as

$$R_x[m] = \langle x[n]x[n-M] \rangle$$

$$\lim_{N->\infty} \frac{1}{2N+1} \sum_{n=-N}^{N} x[n]x[n-M] \qquad (5.4) \quad [7]$$

If x[n] was periodic with period N, then $R_x[0]=R_x[kN]$, where k=1,2,3,…

Therefore, $R_x[kN]$ will always be large in magnitude. If x[n] was not periodic, then this result would not be true. Although, a noiseless signal is not purely periodic ($\frac{Rx[N]}{Rx[0]} \neq 1$), the ratio is still relatively high, while a non-periodic signal has a ratio far below 1.

5.5 Motion Detector

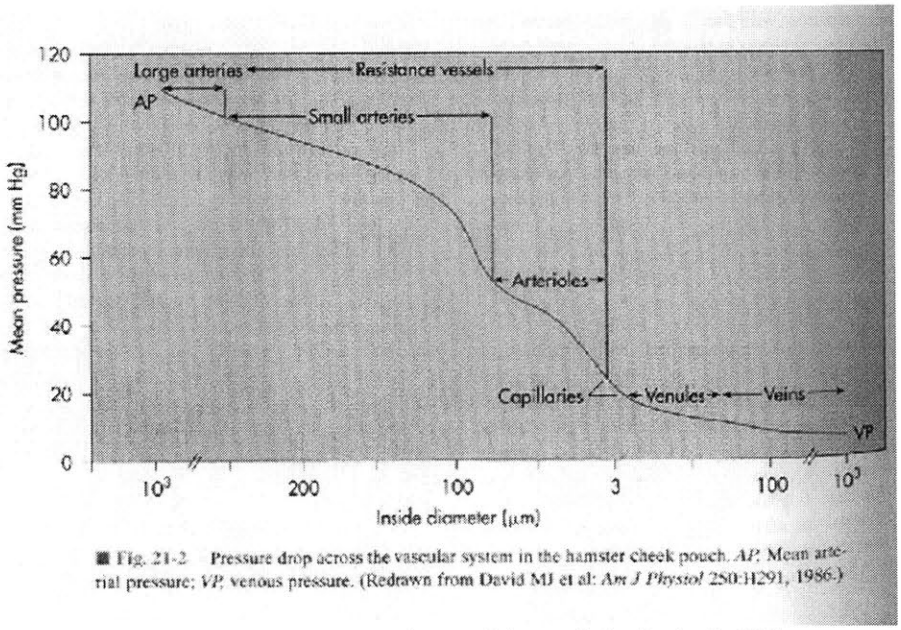

■ Fig. 21-2 Pressure drop across the vascular system in the hamster cheek pouch. *AP*, Mean arterial pressure; *VP*, venous pressure. (Redrawn from David MJ et al: *Am J Physiol* 250:H291, 1986.)

Figure 5.3 Mean pressure of essential vessels in the body [13]

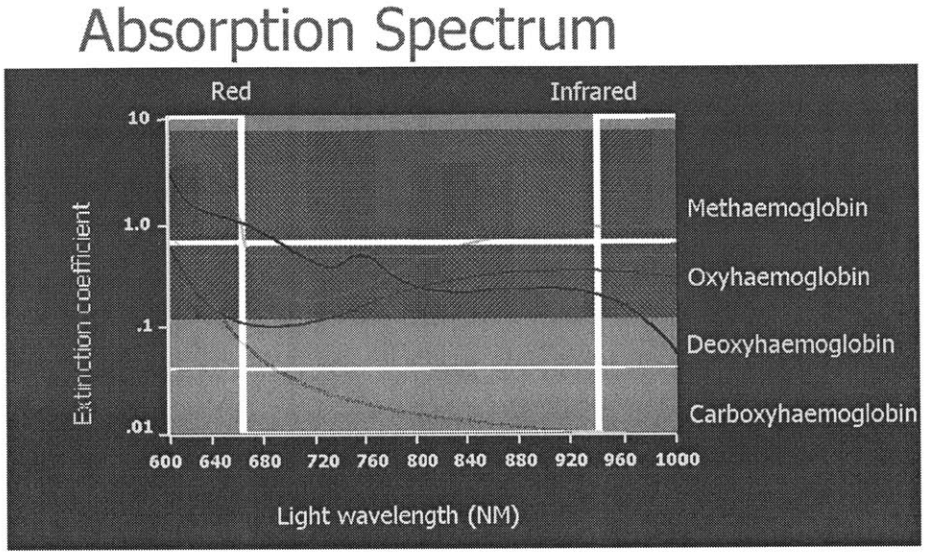

Adapted from:

http://www.health.adelaide.edu.au/paed-anaes/talks/brazil/oxygen/index_files/frame.htm

Figure 5.4 Absorption Spectrum

Revisiting chapter 2, the photodetector picks up both pulsatile and non-pulsatile components from the arteries and capillaries. In addition to these components, the photodetector picks up venous contributions, absorptions from the tissue and the bone. From figure 5.3, it is shown that the artery has significantly more pressure than the vein. Therefore, when undergoing motion, the vein is more susceptible to motion. Ambient light also has more of an influence on the vein. Revisiting the absorption spectrum in figure 5.4, it can be seen that at 660 nm deoxyhaemoglobin has a higher absorption coefficient than oxyhaemologlobin. Therefore, if a 660 nm light source was illuminated through the finger, the photodetector will detect oxyhaenoglobin, but will also pick up a significant amount of deoxyhaemoglobin. Considering the vein carries only deoxygenated blood, then the photodetector will posses a significant contribution from

the vein. If the motion detector can primarily pick up on the contribution due to the vein, then this will serve as a noise reference for the signal. In the previous ring sensor design, the elastic band pressurized the finger at a pressure greater than 20 mmHg, thus eliminating venous contribution. The new design exerts less than 5 mmHg of pressure thus ensuring that the flow through the vein is not interfered with. In addition, the motion photodetector will be placed away from the localized pressure such that the vein is not occluded due to pressure adjustments, then the motion photodetector can be placed in a region where it picks up the vein contribution but is not affected by the localized pressure unit.

5.6 Results of Different Methods

5.6.1 Accelerometer

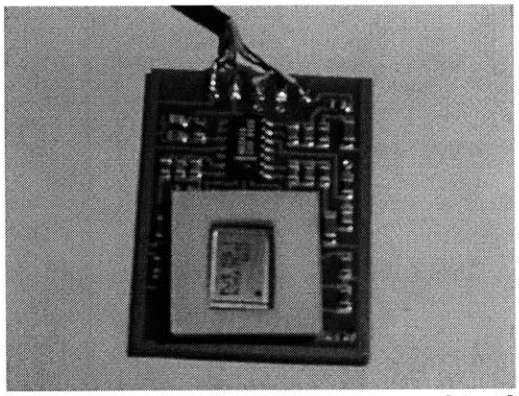

Figure 5.5 ACH 04-08-05 accelerometer and test board

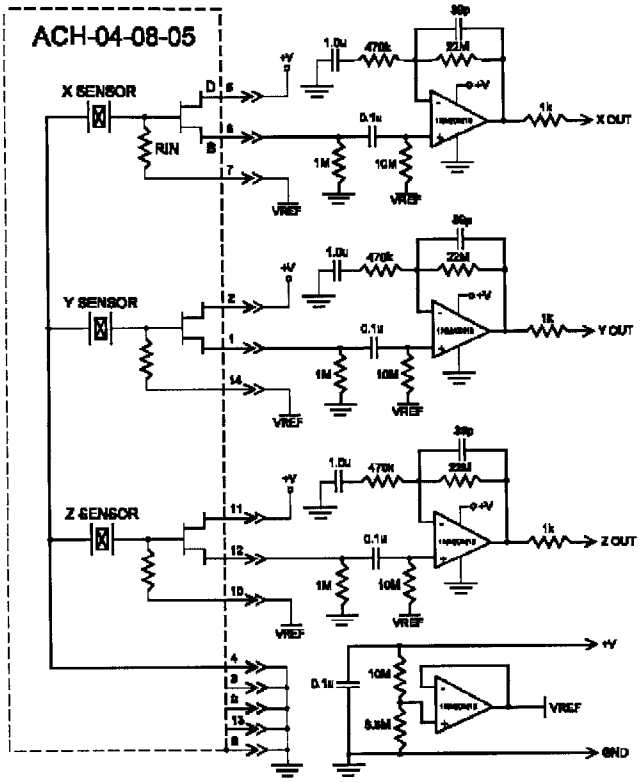

Figure 5.6 Circuit diagram of the accelerometer board

A low power, ACH-04-08-05 accelerometer and its corresponding MSI's Analog Test PCB were used to determine the acceleration of the finger. The specifications sheet given from Measurement Specialties In, informed the customer that it "operates on the principle that its sensing elements are a small cantilever beam consisting of a metal substrate with a piezoelectric polymer element affixed to one side. Each beam is supported at one end while the opposite end is allowed to flex in response to acceleration. The beam flex strains the piezoelectric material, which generates a charge proportional to the applied acceleration".

The Test PCB was 40mm by 30mm, while the sensor alone is only 11.2mm by 8.3mm. Along with being small and flat in size it also possessed 3-axis accelerometer, three simultaneous analog outputs, low frequency response, low-Impedance output, and low cost. The accelerometer was fixed onto the palm of the hand, to measure all actions of the finger, which the hand will undergo too. Though this is not an optimal position for the measurement of bending, it provided a sufficient assessment of the other motion characteristics of the finger due to the coupling between the finger and hand.

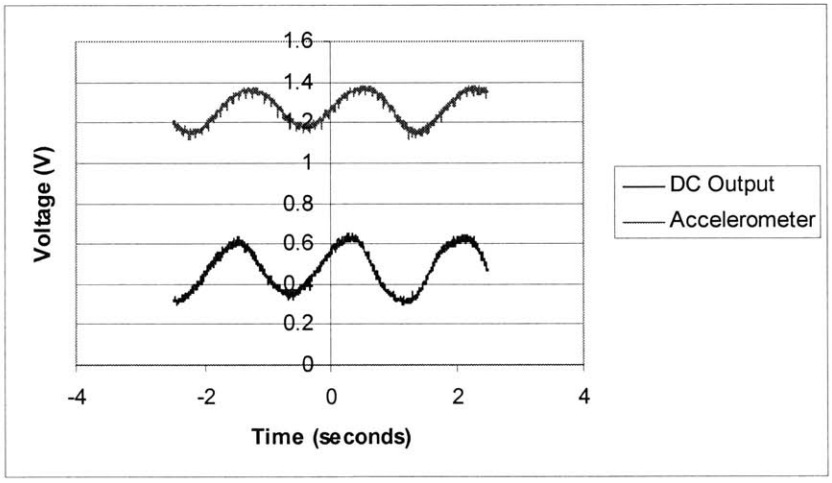

Figure 5.7 Performance of the accelerometer

Looking at the figure 5.7, when the finger undergoes a certain motion, the accelerometer picks up on the change. Thus, observing the amplitude or the frequency response of the accelerometer waveform serve as a motion indicator. After capturing this data, the frequency or amplitude must be compared to some previous established threshold value. If this is above some threshold then motion artifact was present.

This method was very accurate. When motion was present, the sensory unit can detect whether or not motion was detected. Therefore, this was highly accurate with few false alarms and few missed detections. The drawbacks of using an accelerometer were in order to meet size constraints, the signal-processing unit would have to be redesign. In addition, the accelerometer would need more power to amplify its amplifiers. The result, more power consumed by the ring sensor.

5.6.2 Maximum Likelihood Method

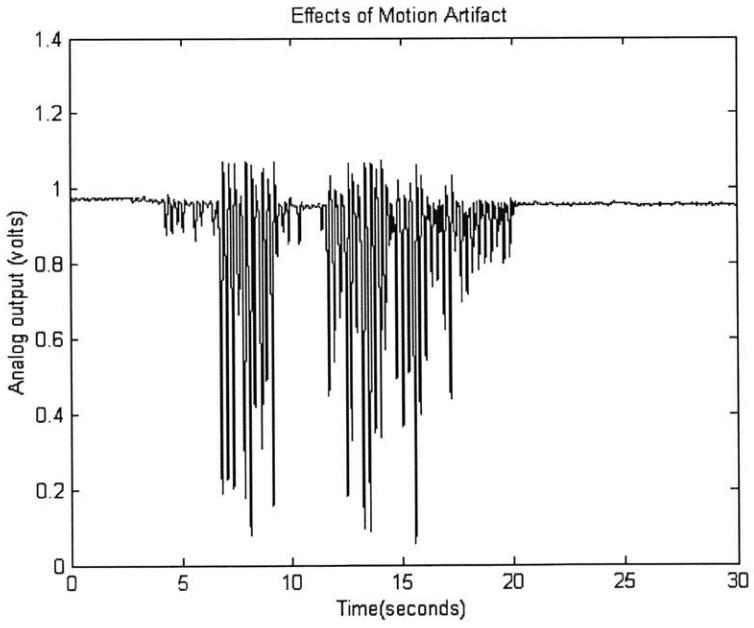

Figure 5.8 Analysis of motion artifact from PPG sensor

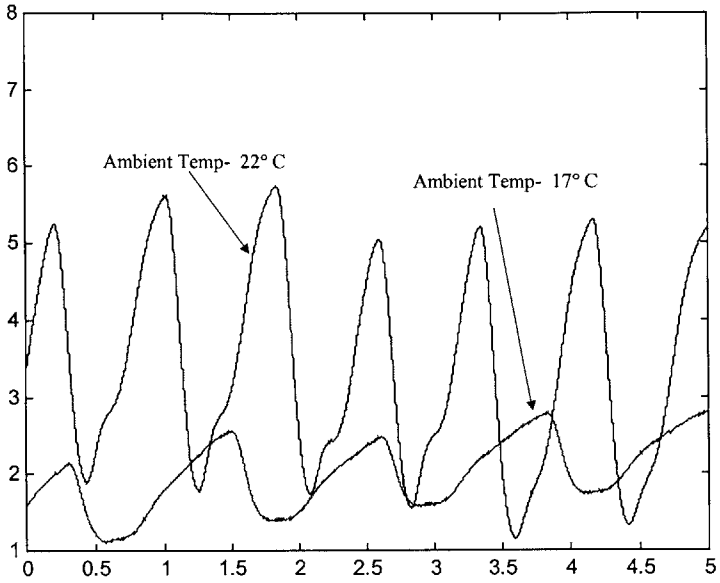

Figure 5.9 Environmental effects

It was sufficient to choose the intensity value as the random variable. Figure 5.8 verified the fact that under motion the amplitude of the signal was significantly higher than that of the pulse signal. External factors such as temperature could also cause the arterial volumetric pulsations to increase (see Figure 5.9). Though, temperature caused the amplitude to increases, it is not as pronounced as motion artifact. This is shown by comparing the factor of amplification of the above figures. Temperature increase resulted in an amplification of 4. When motion was induced, the amplitude of the waveform increased by a factor of 45.

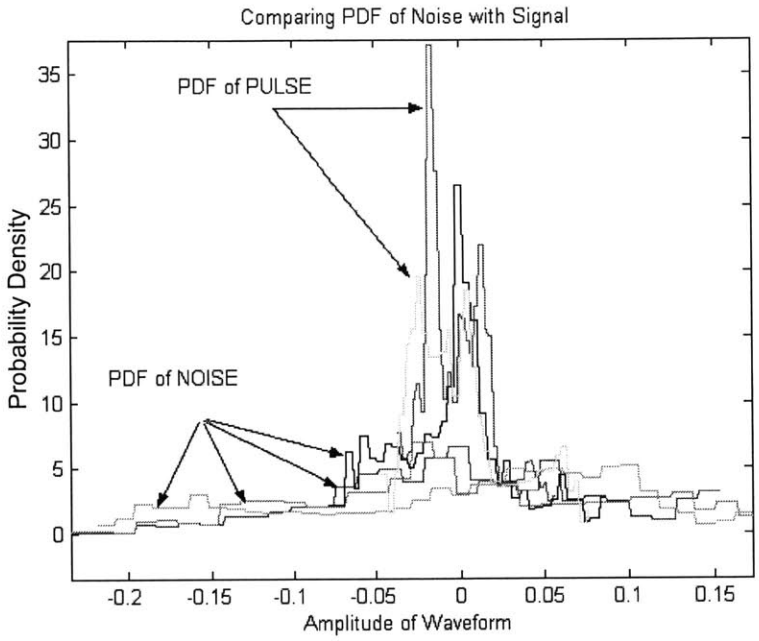

Figure 5.10 Probability density function of pulse and motion signal

Figure 5.10, shows the pdf of a few motion signals and few pure pulse signals. When analyzing this figure, it seemed that it did not fit the Gaussian model. This was due to the small number of trials investigated. If more trials were taken, then by the central limit theorem, the figure would have resembled Gaussian model. Thus, since the two have a different probability model, a threshold value can be computed. Though this method was effective, it might be insufficient on certain types of motion. Depending on the robustness of the photo plethysmographic sensor, small perturbations might be effected. If a small motion was influential, then this approach might not be optimal.

5.6.3 *Autocorrelation Method*

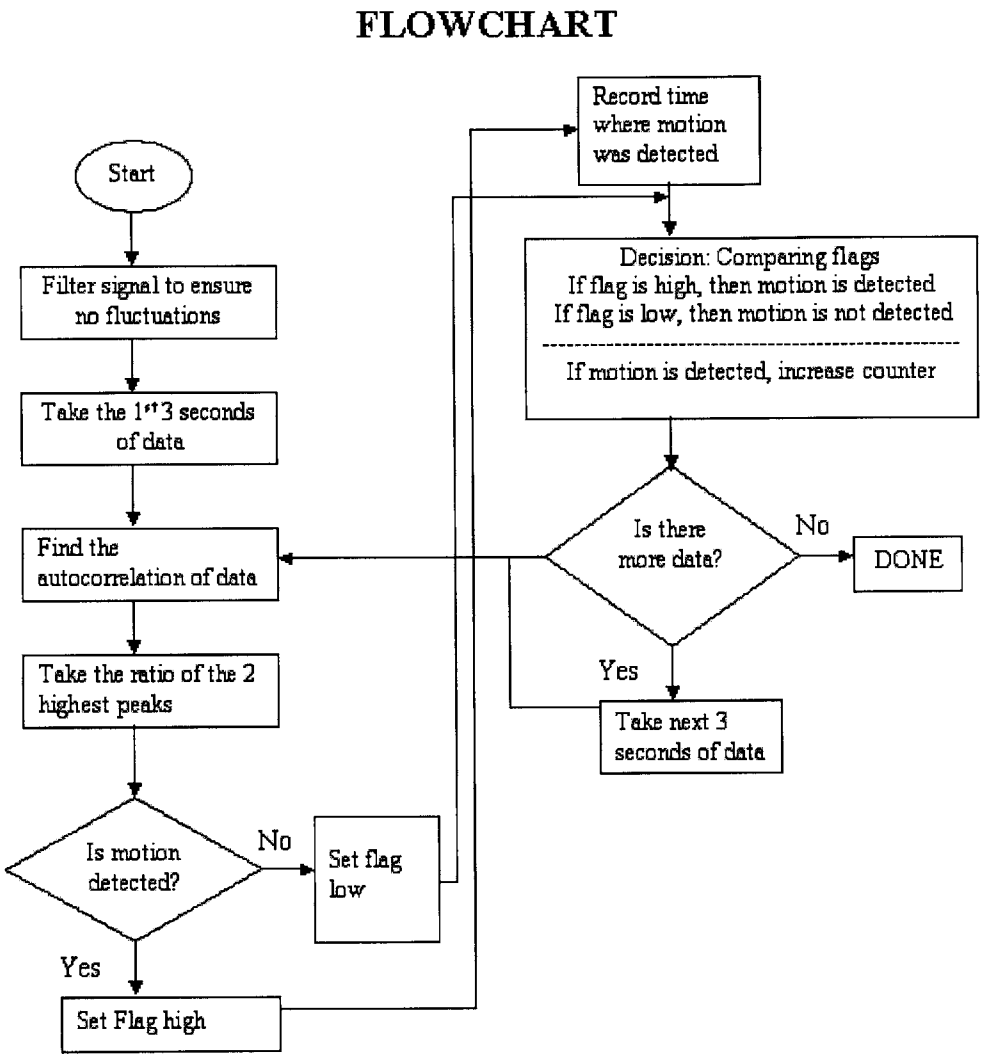

Note: For motion detection algorithm, a 3 second window of data was observed. The autocorrelation was computed for this section of data. The ratio of the 2 highest peaks was acquired. This ratio was compared to a previously established threshold. It was determined if the signal was periodic or not. Assuming a motion will produce a non-periodic signal, then if the ratio was high, motion was detected.

Figure 5.11 Flow chart of motion detection algorithm

The autocorrelation method was used to determine is the signal captured is periodic. The algorithm used has the following characteristics: an automated program for motion detection, locates the regions of motion detection. This detection program was developed for analyst who observes the data offline. If a detection system needed must provide a real-time indicator of detected motion, only slight modifications would have to be done in order to implement this into a continuous monitoring device. A flow chart was of the motion detection algorithm was constructed to outline the important steps of the autocorrelation method. Initially, the algorithm applied a high pass filter to ensure that the DC fluctuations were eliminated from the signal. Next, the first three seconds of data was observed. Though the window can be enlarged, the size was chosen due to further applications of real-time. The autocorrelation was computed for the three second data. The algorithm searched for the two highest peaks stemming from the autocorrelation function. These parameters where recorded and compared. If their ratio was above a certain threshold, then the detection program would indicate there is no motion; if the ratio was below this threshold, the program would detect motion and record the time that event happen. The decision process is clearly shown in the flow chart. After the decision was made the algorithm would see if there was more data. If so, the window captures the next three seconds and the process repeats. The conclusion of the program applying this algorithm, a list of regions total amount of detections and regions of motion should be displayed for the analyst.

Good Signal (ratio 0.68)

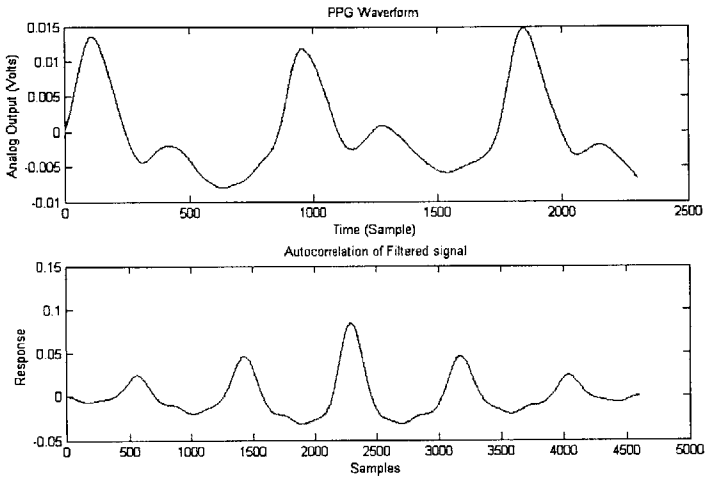

Figure 5.12 Plot of a non-motion signal and corresponding autocorrelation

Motion Influence Signal (ratio 0.15)

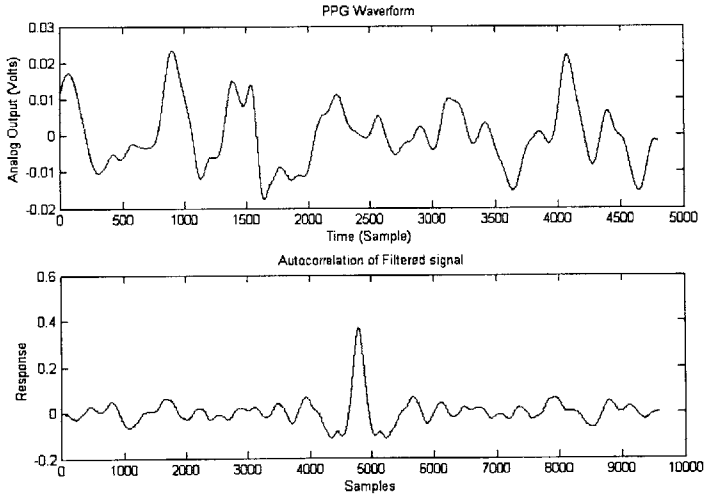

Figure 5.13 Plot of a motion signal and corresponding autocorrelation

In, figure 5.12 shows an example of three second data of a clear pulse signal. Using the motion detection algorithm developed, a result of .68 was yielded which sent no flag, i.e. detected no motion. Figure 5.13 consists primarily of a random noisy signal. Using the motion detection algorithm developed, a ratio of 0.15 was computed. Therefore, the later was flagged by the program and informed the analyst that motion was detected.

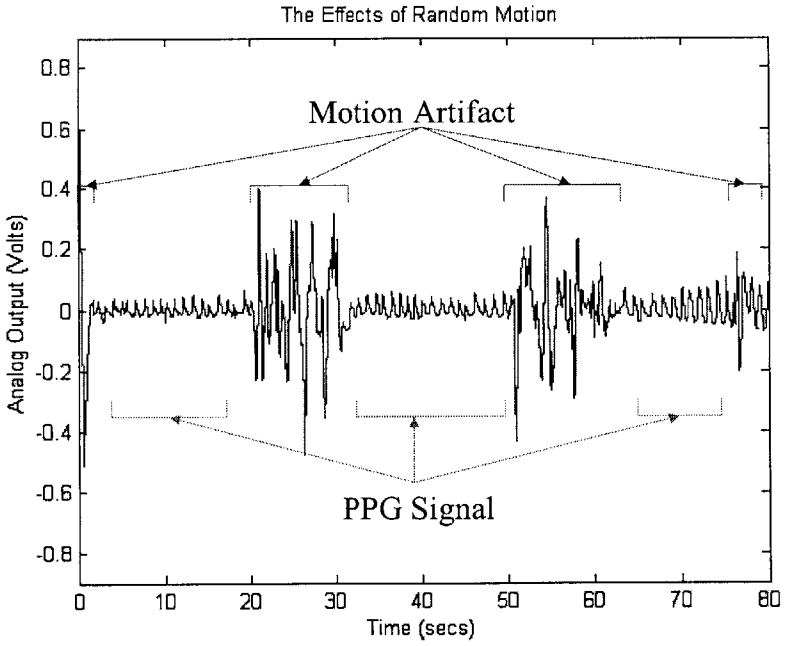

Figure 5.14 Examining the effects of random motion

In order to see how well this detection system worked in practice, a series of measurements were taken. The sensor band was placed around the finger base of a healthy 26 year old male. The subject was still for a period of 20 seconds. Then random motion in the form of gestures and random movement was done for 10 seconds. This process was repeated for another cycle and then ended with the patient remaining still for 20 second. Figure 5.14 shows this plot. Using the automated program for motion detection, motion was detected in various regions. Table 1 shows three regions of detection, false alarms, and missed detection.

Table 5.1 Motion Detection of a Random Motion

Signal	Period of noise (secs)	Period of Detection (secs)	Correct Detection (secs)	False Alarm (secs)	Missed Detection (secs)
samp_motion1	0 to 4	0 to 6	0 to 4	5 to 6	none
	18 to 32	18 to 36	18 to 32	32 to 36	none
	50 to 64	48 - 66	50 to 54	64 to 66	none
	76 to 78	75-80	76 to 78	78 to 80	none

Analyzing the table, it can be shown that both the autocorrelation method and the algorithm used to implement it worked sufficiently. All regions of motion were detected. Though there were a series of false alarms, they only account for 11 seconds of incorrect data. This was due to the algorithm's use of a 3 second window. Thus, most of the false alarms are due to the window possessing motion-influence signal from the previous regions. For example, the when the window was analyzing the segment 3-6 seconds,

though 5^{th} and 6^{th} seconds have a motion-free pulsation, the 4^{th} second still possesses noise, thus the algorithm will still detect noise. Shortening the window will reduce this factor, but there must be a sufficient data in the window such that the autocorrelation function has an enough data points to make an accurate decision. A window of three seconds was chosen, because it was seen that this small window still had the ability to make an accurate decision. Using a short window for detection means, endured motion could be detected in a reasonable time. This is appropriate for real-time monitoring. If solely used for the purpose of long-term monitoring, a longer window would be sufficient because of improvements in accuracy.

The draw back of this method is the influenced of a periodic disturbance. A periodic disturbance can be the result of repetitious vibrations in the environment, continuous gestures, or jogging at a certain pace. If the periodic disturbance is outside the bandwidth of interest, then classical filtering techniques can be used to filter out this disturbance. Unfortunately, if the periodic noise is close to the periodicity of the pulse, the disturbance cannot be filtered. Therefore, the autocorrelation method would be ineffective.

To observe the inefficiency of periodic motion, a couple of cases (bending and tapping) were examined.

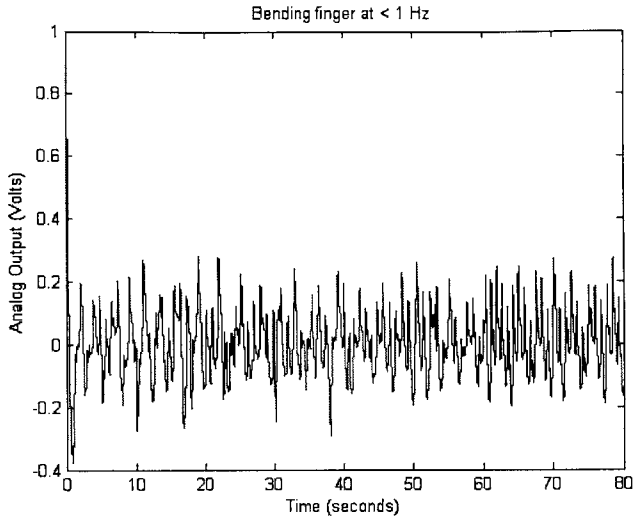

Figure 5.15 Finger bent less Than 1 Hz

Table 5.2 Motion Detection of a Finger Bent Less Than 1 Hz

Signal	Period of noise (secs)	Period of Detection (secs)	Correct Detection (secs)	False Alarm (secs)	Missed Detection (secs)
bend1s	0 to 80	0 to 60	0 to 60	none	60 to 72
		72 to 75	72 to 75	none	75 to 80

When the finger undergoes periodic bending the finger less than one Hz, there were no false alarms but there are a series of miss detections. Though this consisted of 20% of the data, yet it was significant (Figure 5.15, Table 5.2).

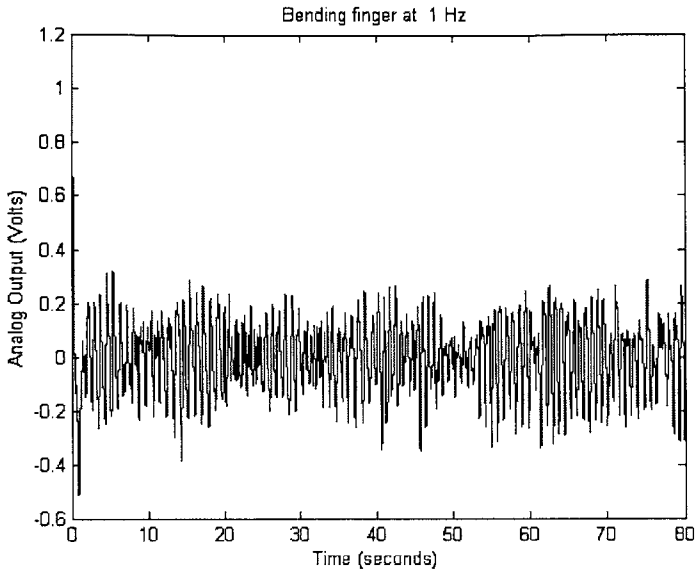

Figure 5.16 Finger bent at 1 Hz

Table 5.3 Motion Detection of a Finger Bent at 1 Hz

Signal	Period of noise (secs)	Period of Detection (secs)	Correct Detection (secs)	False Alarm (secs)	Missed Detection (secs)
bend1f	0 to 80	0 to 3	0 to 3	none	3 to 9
		9 to 12	9 to 12	none	12 to 18
		18 to 21	18 to 21	none	21 to 48
		48 to 51	48 to 51	none	51 to 74
		75 to 80	75 to 80	none	

Increasing the bending rate to approximately in the same bandwidth as the pulse (1 Hz), it was shown that there are no false alarms, but there were a series of miss detections. Miss detections consisted of 77.5% of the data (Figure 5.16, Table 5.3).

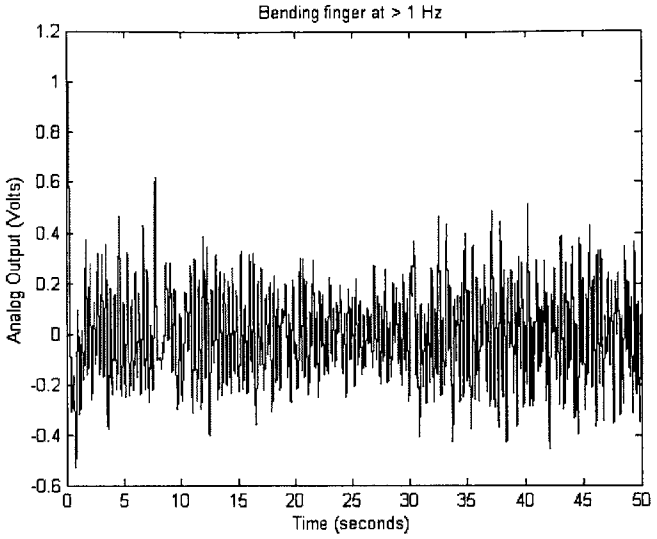

Figure 5.17 Finger bent greater than 1 Hz

Table 5.4 Motion Detection of a Finger Bent Greater Than 1 Hz

Signal	Period of noise (secs)	Period of Detection (secs)	Correct Detection (secs)	False Alarm (secs)	Missed Detection (secs)
bend1ff	0 to 50	0 to 3	0 to 3	none	6 to 18
		18 to 21	18 to 21	none	21 to 39
		39 to 45	39 to 45	none	45 to 50

In figure 5.17, the finger was bent at a rate above 1 Hz, there were a no false alarms, but again there are series of miss detections. Table 5.4 shows that miss detections consisted of 70% of the data.

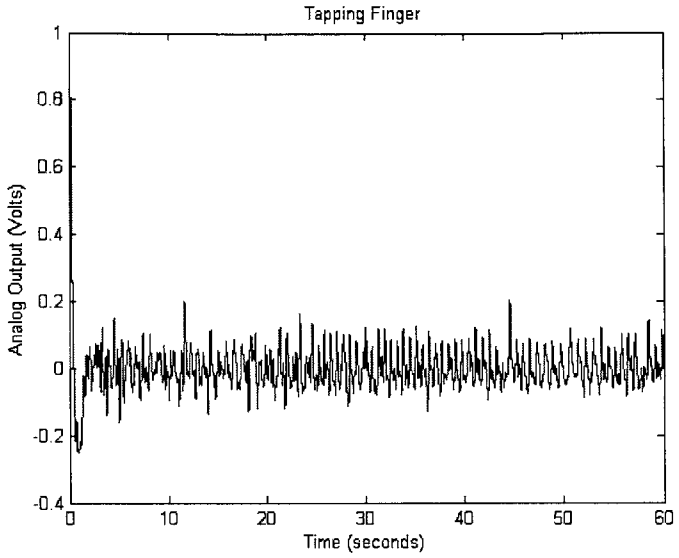

Figure 5.18 Finger tapped on a flat surface

Table 5.5 Motion Detection of a Finger Tapped on a Flat Surface

Signal	Period of noise (secs)	Period of Detection (secs)	Correct Detection (secs)	False Alarm (secs)	Missed Detection (secs)
tap1	0 to 60	0 to 3	0 to 3	none	3 to 9
		9 to 12	9 to 12	none	12 to 18
		18 to 21	18 to 21	none	21 to 42
		42 to 45	42 to 45	none	45 to 60

When observing another mechanism of motion, tapping, it was seen that there were no false alarms but there were miss detections. This consisted of 80 % of the data (Figure 5.18, Table 5.5).

5.6.4 Motion Detector

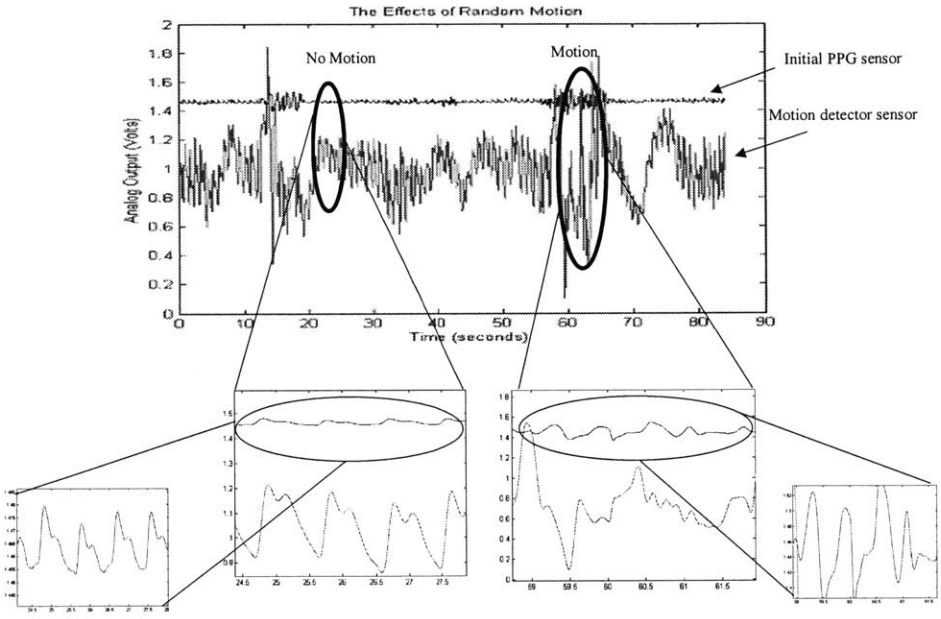

Figure 5.19 Motion detector and photodetector signal

The new sensor band consisting of the motion detector was applied to the finger base. Recall, the sensor band consisted of two photodetectors and 2 LEDs. The original photodetector (PPG sensor) captures the volumetric pulsations of a patient. The 2nd photodetector (motion detector) captures the venous contribution. In Figure 5.19, the motion detector was compares with the photo plethysmograph detector. When observing the data, the second photodetector possessed a larger amplitude than the PPG detector in all regions. This was due for various reasons:

1) The photodetectors were different. Each photodetector had a different response.

2) The gains on the two circuits were different.
3) The motion detector was closer to the light source thus it was expected to have larger amplitude.

Most of these variables can be adjusted by a scaling factor. The motion detection was designed to measure the venous contribution. Though veins do not pulsate, the waveform shows pulsations from both detectors. This was due to the capillary pulsations. Because of the location the capillaries laid on the surface of the finger and its comparable occlusion pressure to vein, it was difficult to separate the contribution of the capillaries. Therefore, these pulsations were deemed acceptable if the motion detector could still provide an accurate detection of motion. Therefore, when comparing the two sensors, the pulse wave was shown on both sensors. Both sensors displayed the trough and crest of the waveform and the dicrotic notch during periods of non-motion. When motion was present, the two sensors showed two different responses. The motion detector was susceptive to motion. Therefore, the motion detector is an indicator if motion is present in the signal.

In combing the autocorrelation method to the motion detector method (using the data from 5.19), it was observed that the motion detector obtains more regions of motion.

Table 5.6 PPG Detector

Signal	Period of noise (secs)	Period of Detection (secs)	Correct Detection (secs)	False Alarm (secs)	Missed Detection (secs)
test2	0 to 3	0 to 3	0 to 3		
PPG detector		6 to 9		6 to 9	
	12 to 21	15 to 21	12 to 21		12 to 15
	32 to 44	27 to 33	32 to 33	27 to 32	33 to 36
		36 to 45	36 to 44	44 to 45	
	55 to 68	54 to 57	55 to 57	54 to 55	57 to 60
		60 to 63	60 to 63		63 to 66
		66 to 69	66 to 68	68 to 69	
		75 to 81		75 to 81	

Table 5.7 Motion Detector Table

Signal	Period of noise (secs)	Period of Detection (secs)	Correct Detection (secs)	False Alarm (secs)	Missed Detection (secs)
test2	0 to 3	0 to 9	0 to 3	3 to 9	
Motion Detector	12 to 21	`12 to 21	12 to 21		
	32 to 44	27 to 33	32 to 33		33 to 39
		39 to 45	39 to 44	44 to 45	
	55 to 68	57 to 66	57 to 66		55 to 57
		75 to 81		75 to 81	

One noticeable difference was the motion detector reduced in the motion number of missed detections. These missed detections comprised of 8% of the total signal while using the algorithm on only the original photodetector, we have missed detections consisting of 13% of the data.

Therefore, the data shows, that when combining the autocorrelation algorithm with the motion detector, it detected more motion influence from this photodetector. This was due to the theory that the motion detector was more susceptive to motion. Thus, using a combination of the two methods a more reliable unit can be constructed.

CHAPTER 6
RING MONITORING SYSTEM

6.1 Introduction

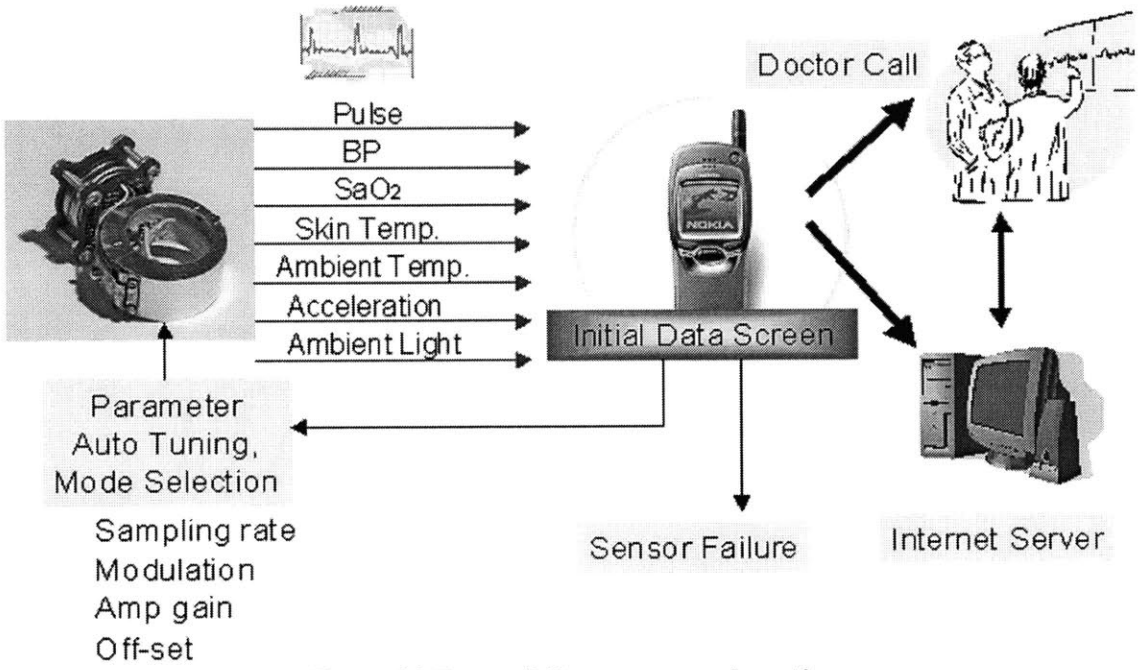

Figure 6.1 Data validity assurance schematic

Along with the ring sensor a Personal Digital Assistant (PDA), laptop, or desktop is used to record and display pertinent information. Each interface has an application that has the ability to capture and save the data. Some applications provide additional signal processing to filter additional noise received during the transmission state. This architecture has the potential of closed loop control. Therefore, using the parameters

obtained by different sensors, the system has the ability to adjust itself such that it can accommodate for environmental or physiological changes. Also, it will evaluate the patient and either submits the data to the Internet server or alert a medical professional given the status (Figure 6.1). To obtain additional information from the patient and the environment, additional sensors are applied to ring. In this section, discussion will be focused on the ring monitoring system. Both the sensors and the display unit will be discussed.

6.2 Additional Sensor Components

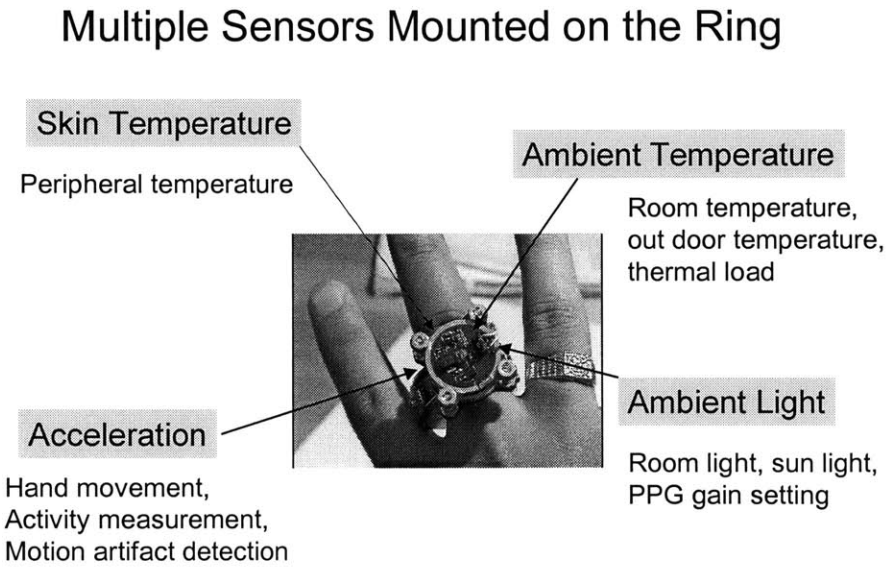

Figure 6.2 Additional sensors

Adding a series of sensors onto the ring sensor will enable the sensory unit to monitor more aspects regarding the status of an individual and the environment. Four

sensors have been added to the sensory unit: a cadmium sulfide sensor to monitor the ambient intensity of light, two thermistors to monitor skin temperature and ambient temperature, and a "motion detector" used to detect motion artifact. The latter has been discussed in the previous chapter.

Cadmium Sulfide photocell

Research on cadmium sulfide (CDS) materials has been ongoing for 70 years. A CDS photocell is photo resistor, made by depositing doped cadmium sulfide on a ceramic substrate [22]. These sensors change their resistance values based on the exposed intensity of light. Due to these sensors ability to measure the light intensity accurately, they are commonly used in the photography industry. With the ability to measure light intensity, the industry can adjust their shutter speed on a camera used in their field to ensure maximum quality. Therefore, using a CDS cell will enable the ring sensor to monitor the intensity of ambient light.

Thermistors

To observe the ambient temperature and the skin temperature, two thermistors were added to the ring sensor. Thermistors (thermal resistors) are temperature sensitive passive semiconductors, which exhibit a large change in electrical resistance when subjected to a relatively minute change in body temperature. They provide stability, accurate measurements, and extremely sensitive to minute temperature changes.. Two Negative Temperature Coefficient (NTC) thermistors were added to the ring sensor unit. One thermistor was used to monitor skin temperature while the second was used to

monitor ambient temperature. When subjected to an increase in temperature, the thermistors decrease in resistance.

6.3 Implementation

6.3.1 *Cadmium Sulfide Photocell*

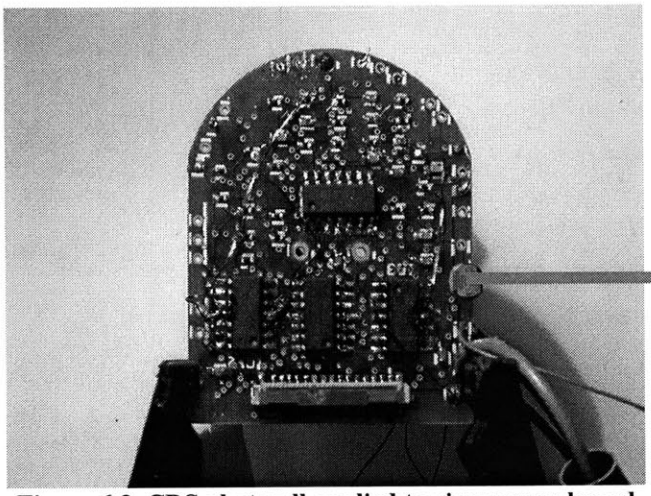

Figure 6.3 CDS photocell applied to ring sensor board

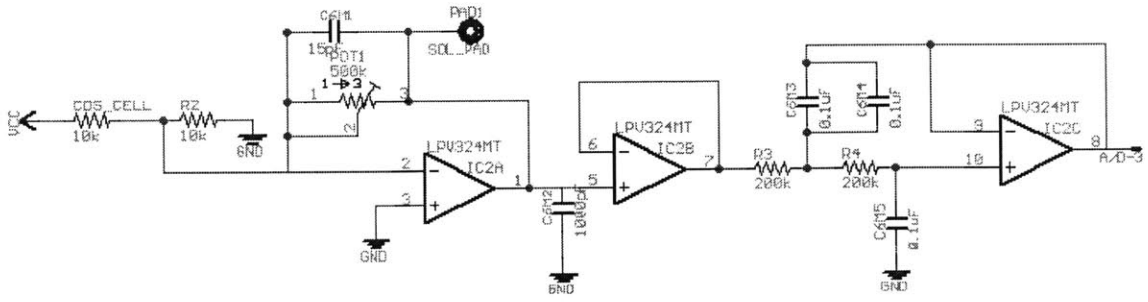

Figure 6.4 Circuit diagram of CDS photocell and filter

Using a cadmium sulfide (CDS) photocell of 10k ohms, we are able to detect the intensity of the ambient light was measured. The CDS sensor was included into the circuit such that an analog voltage was generated. This voltage passed through a filter to eliminate electromagnetic effects due to the indoor lights. Figure 6.3 shows this CDS cell. Figure 6.4 shows the circuit design.

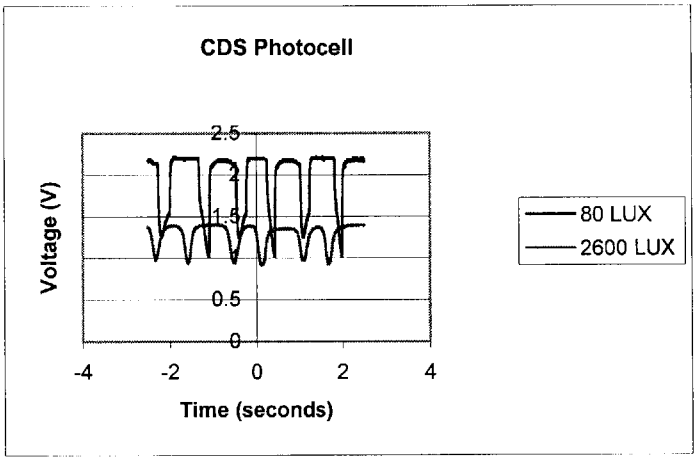

Figure 6.5 Experimental results of CDS sensor

Experimental measurements were done to observe the CDS sensor's response to different intensities of light. In Figure 6.5, the sensor was moved in and out of the 80 and 2600 LUX light levels. As the data suggested, the CDS sensor an detect different light intensities.

6.3.2 NTC Thermistor

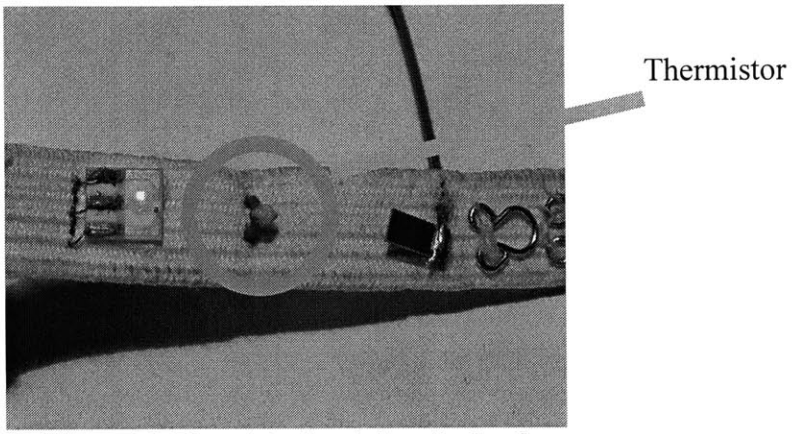

Figure 6.6 Thermistor located on the band

Two thermistors were added to the sensor to provide information about the ambient and skin temperature. Using 10 kΩ thermistors (@ 25 °C), generated a current of 100 μA. This resulted in minimal power consumed. Figures 6.6 shows the thermistor..

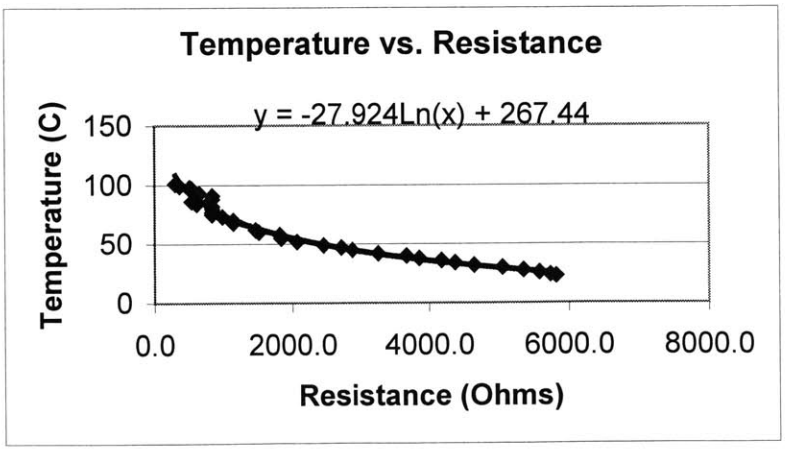

Figures 6.7 Calibration of the thermistor

Using a hot plate, beaker, and thermometer, the thermistor was calibrated. The beaker was initially filled with crushed ice. The beaker was placed on the hot plate. The thermistor and the thermometer were placed in a manner where both where impeded in the ice, but did not reside on the base or the sides of the beaker. The hot plate's temperature was slowly adjusted to ensure an accurate reading. Both temperature and the resistance were recorded. Figure 6.7 shows the calibrated data.

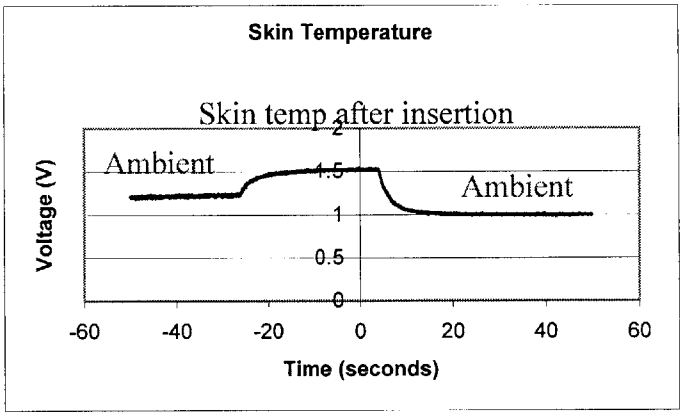

Figure 6.8: Hand immersed in 18 °C H_20

Experiments were done to observe the behavior of the finger under different environments. The band in Figure 6.6 was applied to the base of the finger. The thermistor was recorded with the finger at room temperature for approximately 20 seconds. Then the hand was immersed in a 18 °C ice bath for another 20 seconds. For the remainder of the time the hand was taken out of the ice bath. The experimental data shows that when the finger was subjected to a colder environment, the thermistor registered a change. When the finger was taken out of the ice bath, the finger regains the

previous temperature. Figure 6.8 shows these results. Therefore, using a thermistor, an initial assessment of vasoconstriction can be made.

6.4 Ring Monitoring System

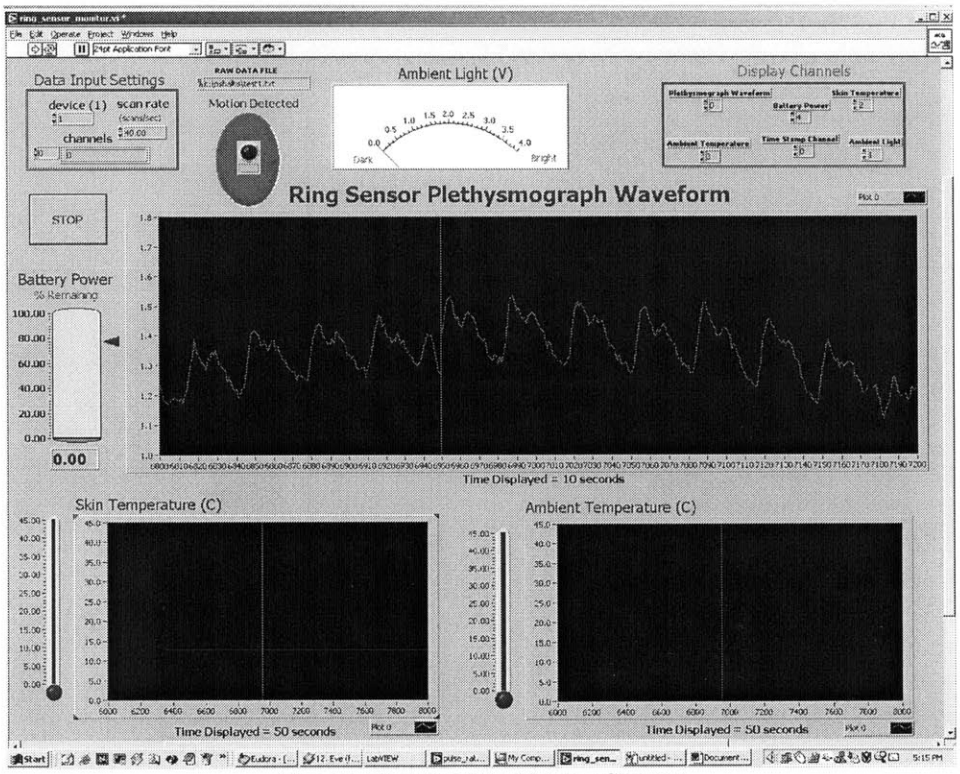

Figure 6.9 Ring Monitoring System

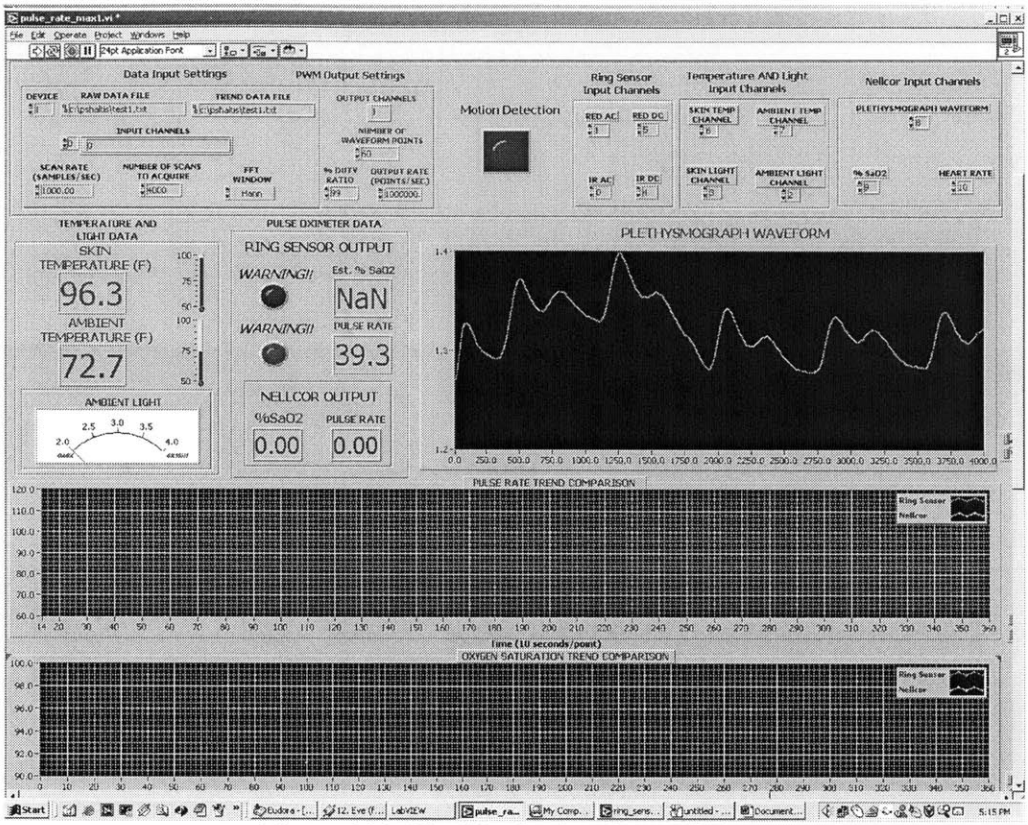

Figure 6.10 Ring Monitoring System Deluxe

The monitoring system for the ring sensor has been in continuously changing in recent years. Previous interfaces such the display program provided by Sokwoo Rhee, used a C++ program to display the program. This program showed real-time data, saved the data, and showed pulse history. A PDA was also used to enable the user to be completely mobile. Recently, Phil Shaltis, a graduate student, developed a labview program, shown in Figure 6.9. This program encompasses the following information: real-time pulse waveform, ambient temperature, skin temperature, battery life, and a motion detector. It also gives the user flexibility in specifying the name and location of the experimental data, the time scale of the pulse window, and sampling rate. A similar

program was also written to enable the operator to compare different devices (see Figure 6.10). It displayed the above parameters with the exception of battery life. Note: battery life assumes that the device is wireless. If the ring sensor is wired, then this indicator is irrelevant. In addition, this program displays the pulse rate history, the blood oxygen saturation history, and other device's (Nellcor in this case) pulse rate, blood oxygen rate, and pulse waveform.

Both these monitoring systems were used in this research to obtain information from the user. The signal-processing unit of the sensory unit was transferred the information to the computer by way of a National Instrument's A/D converter. The display unit applied some additional processing on the data and displayed it. It also saved the data to the disk, such that offline analysis could be done. The data captured from this research was by way of the Ring Monitoring System.

CHAPTER 7
CONCLUSIONS AND RECOMMENDATIONS

A method for signal improvement without circulation interference and a method for motion detection for ring sensors have been presented. The main results of this thesis are discussed below.

The new ring sensor designed provides the same features as the previous design. It allows the optical sensors to be decoupled from the housing unit, maintains size and power constraints, compares in weight. The new sensor also alleviates discomfort caused by the ring sensor's potential to pinch the wearer or to cause ischemia due to the tight elastic band. This unit also protects the sensors from external forces, shields ambient light, and reduces motion artifact.

The new sensory unit improves the signal-to-noise ratio. This was accomplished by providing a localized pressure on a small area of the finger base, thus allowing the blood flow to be unobstructed. This method was compared to a traditional an arm and a finger cuff. By experimental verification, it was proven that although these methods had the ability to improve the signal-to-noise, both the arm and the finger cuff caused the flow to become hindered. The new design showed no circulation interference.

Different techniques for motion detection were presented. An autocorrelation method was decided because of its performance and ability to maintain size and power constraints. Initial results of a 2^{nd} photodetector showed that it could be used as a detection method.

Recommendations

Though the wires were managed in a way, there are still problems with the wires. An improved design of the signal-processing board fastening onto the board will provide a method where, the wires will not be exposed, thus reducing the frequency of outside interference. Thus, the connection between the sensor band and the signal-processing unit will remain intact.

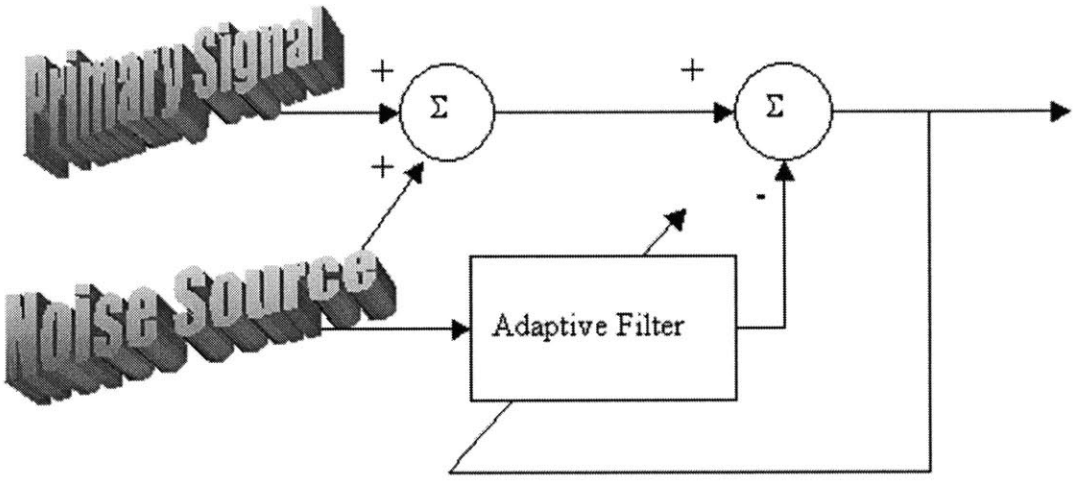

Figure 7.1 Adaptive Noise Canceller

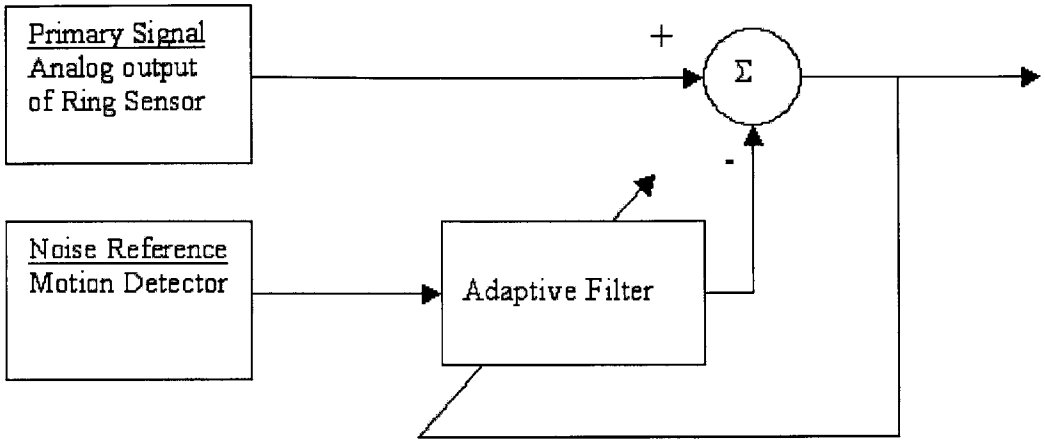

Figure 7.2 Adaptive Noise Canceller (specified)

The motion detector has been proven that it has the ability to detect motion. If the sensor can be placed closely to the vein, then a better noise reference can be obtain, thus making the detection system more reliable. Therefore, a method has to be developed to quickly access if the sensor is in the optimal place. If this location is found, then the second photodetector can be an accurate noise reference. Therefore, using adaptive noise cancellation techniques, the motion artifact can be reduced. Adaptive noise cancellation techniques require two inputs, a primary signal and a noise reference, as shown in Figure 7.1. The primary signal consists of the pure signal and contributions due to noise. In the case of the ring sensor, only the primary signal is known. With the addition of the motion detector and assuming it is an accurate noise reference, then applying this to the noise canceller a significant portion of the noise to become eliminated, thus reducing the motion artifact. (Figure 7.2).

APPENDIX A.1
Software Code

motion_detect.m

```
function [motion] = motion_detect(x)
% motion_detet  Performs motion detection on a ppg waveform
%
%      motion = m_detect(x,lim1,offset);
%          x is vector containing frame of PPG data

% First, remove the dc value of the frame by subtracting the mean . . .

x = x-mean(x);

% Then find the minimum and maximum samples and center clip to
% 75% of those values (`cclip') . . .

maxval=max(x)*.75;
minval=min(x)*.75;

y=cclip(x,minval,maxval);

% CCLIP          performs center clipping of signal
%        y = cclip(x,minval,maxval) center clips the signal in x.
%        Minval must be negative and maxval must be positive.
%        Each elements of x is treated as follows:
%                If x(i) > maxval, then y(i) = x(i) - maxval;
%                If minval < x(i) < maxval, then y(i) = 0;
%        If x(i) < minval, then y(i) = x(i) - minval;

% Compute the autocorrelation of the frame . . .
autocord_y= xcorr(x);

% Find the maximum peak following Rx[0] (`peak') . . .
%Find the first maximum point which should be R[0]
[Max1,I1]=max(autocord_y);

[Max2,I2]=peak(autocord_y(I1:length(autocord_y)));
% Detects next largest value
% where function PEAK  Detects value and index of peak in autocorrelation function.
%        [peakval peakindex] = peak(x) locates the value and index of the
%        largest peak in the vector x other than Rx[0].  x must be an
%        autocorrelation function with maximum value Rx[0] its first element.

%  since R[0] as to be first element, we start with I1
%  and continue until we are at the end of the data (length(autocord_y))


% If ratio is less than 0.33, call then motion occurs
```

```
% otherwise compute no noise is detected  . . .

if Max2 < Max1*.33
   motion=1;
else
   motion = 0;
end
```

run_detect.m

```
function det=run_detect(data)

%  det=run_detect(data)  isa program which is used to find
%     the regions of motion ocurence
%        data is vector containing the data of PPG data

%3 second window equivalent to 3*1000= 3000 Samples, where 1000 is sampling freq.

Fs=1000;            %sampling frequenct
T=3;               %window size
N=T*Fs;             %computes number of samples
counter=0;          %initalizing counter to zero


end_lim=length(data)/N; %computes timne of end of data
for k=1:end_lim
                %moves the window region
win_data=data((k-1)*N+1:(k)*N);
                %uses motion_detect function to find the
                %access if motion exists
if (m_detect(win_data)==1);
                %increase occuerences of motion regions
counter= counter+m_detect(win_data);
                % ocates regions of motion for analyst
sprintf('K =  %d, Time %d',k,((k-1)*N)/Fs)
end



end

counter;            %displays number of 3 second regions with motion
counter*3;          %displays total amounnt of time for region of motion
counter*3/end_lim;     %calculates total percentage of regions of motion
```

plotauto.m

```
function [void] = plotauto(x)
% PLOTAUTO  Plots the autocorrelation function of PPG signal
%
%     plotauto(x);
%        x is vector containing segment of PPG data
%     only plots generated...no value is given

%  Further processing on signal to eliminate noise

%  Using 4th order low-pass Butterworth of cut off of 10 Hz
[B,A]=butter(4,10/500);
sig=filter(B,A,x);

%  Using 2nd order high-pass Buttersworth filter of .5 Hz
[Bh,Ah]=butter(2,0.001,'high');
new=filter(Bh,Ah,sig);

% First, remove the dc value of the frame by subtracting the mean . . .
new-new-mean(new);

figure

plot(1000*(0:1/1000:(length(new)/1000)-1/1000),new)
xlabel('Time (msec)')
ylabel('Analog output (Volts)')
title('Signal')

figure(3)
subplot(211)
plot(xcorr(new));
xlabel('Samples')
ylabel('Response ')
title('Autocorrelation of Signal')
```

HISTPDF.m (taken from 6.555 class)

```
function Density = HistPDF(Intensity, TrainingData, NumBins)

% HIST  Histogram.
%    N = HIST(Y) bins the elements of Y into 10 equally spaced containers
%    and returns the number of elements in each container.  If Y is a
%    matrix, HIST works down the columns.
%    [N,X] = HIST(...) also returns the position of the bin centers in X.


  % TotalCount holds the number of data points in the training data.
  TotalCount = length(TrainingData);

  % BinCounts holds the number of data values that correspond each bin,
  % while BinCenters hold the coordinate of the center of each bin.
  % (again, you might look at the matlab function "hist"



  [BinCounts, BinCenters] = hist(TrainingData,NumBins);

  % BinWidth corresponds to the width of the bins.
  BinWidth     = BinCenters(2) - BinCenters(1);

  % IntensityLow has a value corresponding to the left edge of the leftmost bin
  IntensityLow = BinCenters(1) - BinWidth/2;

  % Loop over the intensity values that are input to this implementation
  % of a hisogram based PDF.
  RetrievedCounts(1:length(Intensity)) = 0;
  for i = 1 : length(Intensity)
    index = 1 + floor((Intensity(i) - IntensityLow) / BinWidth);
    if (index >=  1) & (index <= size(BinCounts,2))
  RetrievedCounts(i) = BinCounts(index);
    end
  end

   % Establish a normalization of the returned PDF values such that
  % the PDF being implemented integrates to one.
  Normalization = 1/(TotalCount*BinWidth);

  % Return the probability density corresponding to the input intensity
  Density = Normalization * RetrievedCounts;
```

run_pdf.m

```
function [void2] = run_pdf(x,xlim1,xlim2)

%  run_pdf(x,xlim1,xlim2)
%  x is the vetor of the PpG waveform
%  xlim1 is the starting point of the data
%  xlim2 is the end limit of the data

% Filtered before entering function
% Used to contrive the pdf and lot it...must specify region of data
% Function used for MLM detetion method


 x=x(xlim1:xlim2);

ylim2=max(x);
ylim1=min(x);

% here is an example of plotting our PDF
 IntensityValues = [ylim1:0.001:ylim2];
% k turns out to be the bum of bins used
% found k=23 to be optimal choice
k=35;
% for k=5:15:300
%    figure


figure(k+4)
plot( IntensityValues, HistPDF(IntensityValues, x, k),'b')
%
% end
```

APPENDIX B.1
Drawings and Images

DRAWINGS OF NEW COMPONENTS

COVER

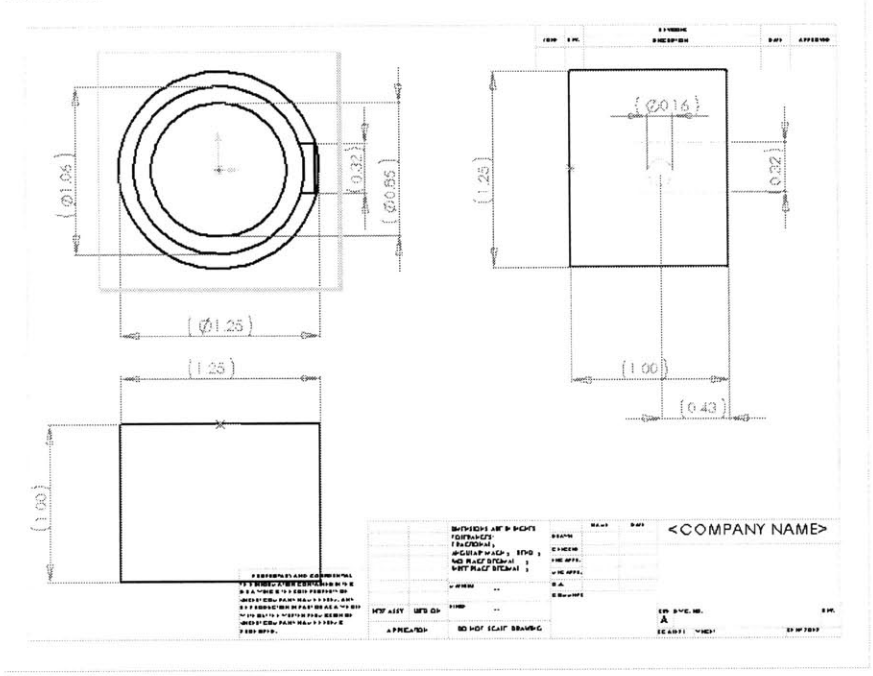

Base

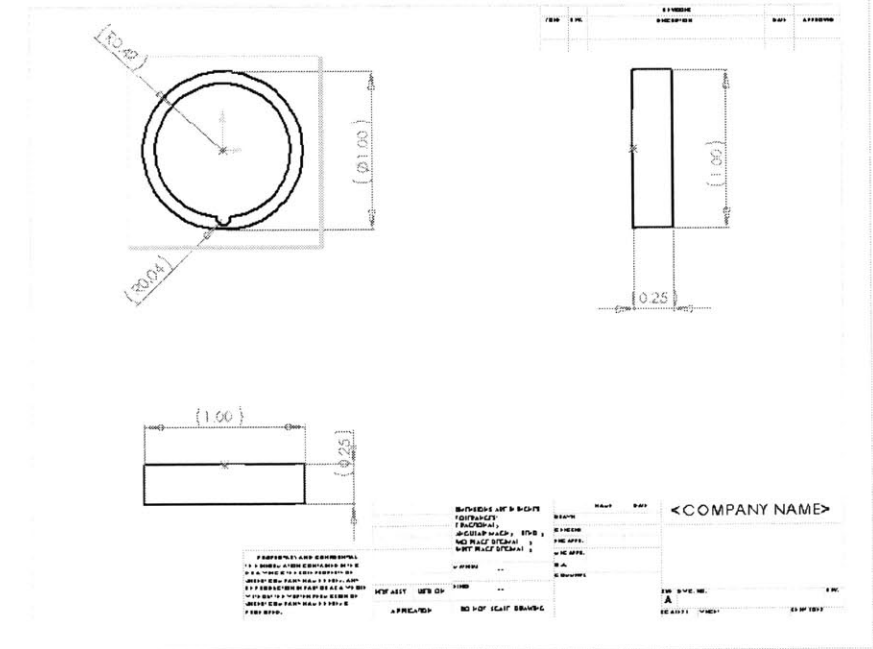

Pressure Band

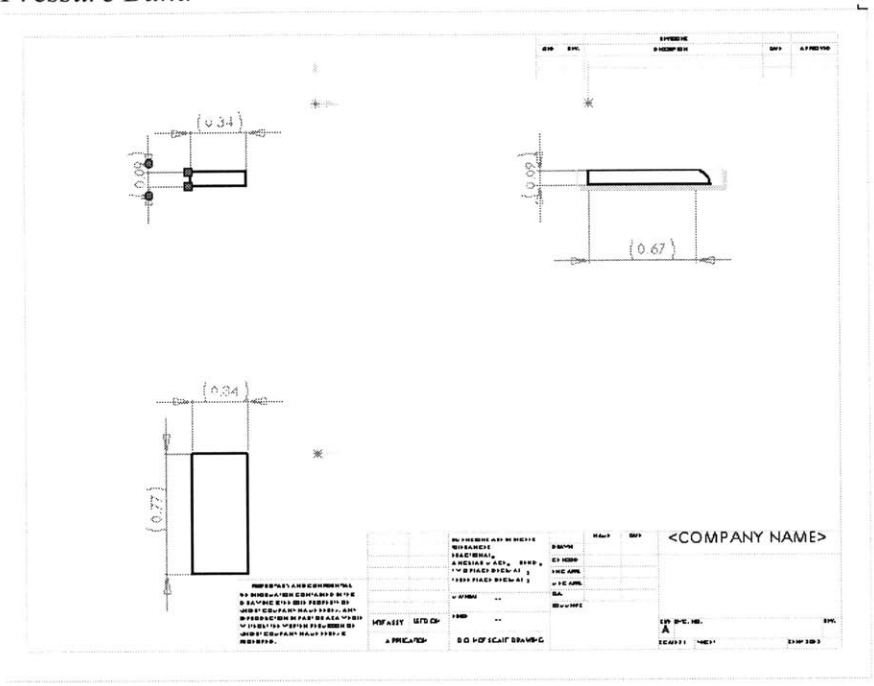

APPENDIX B.2
Drawings and Images

PRESSURIZER AND EQUIPMENT

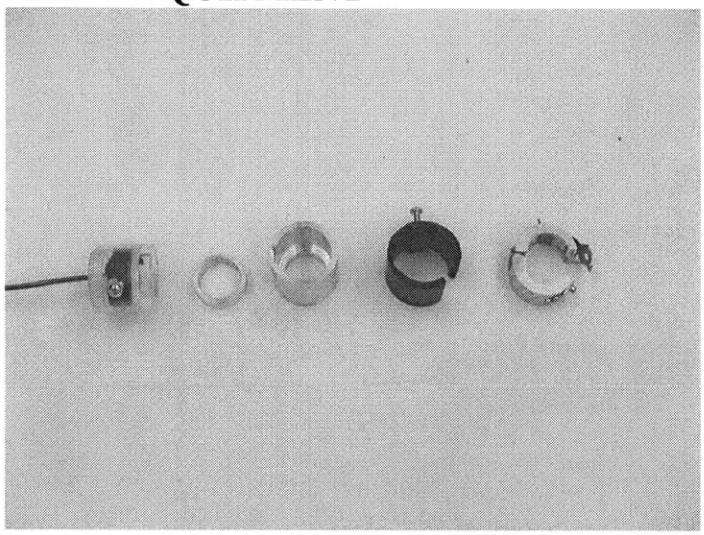

Evolution of Pressurizer

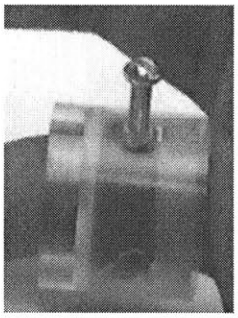

Applying Pressurizer

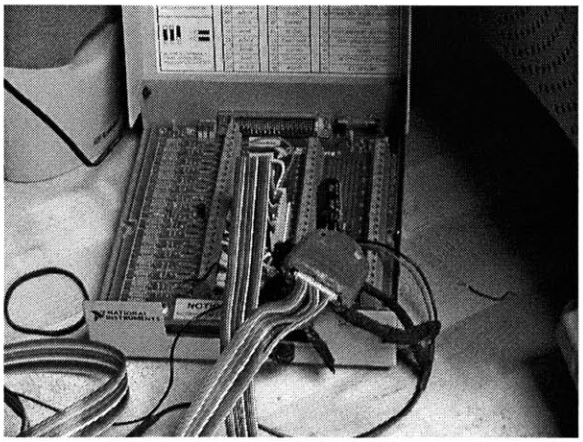

National Instruments Interface board to A/D converter and Ring sensor

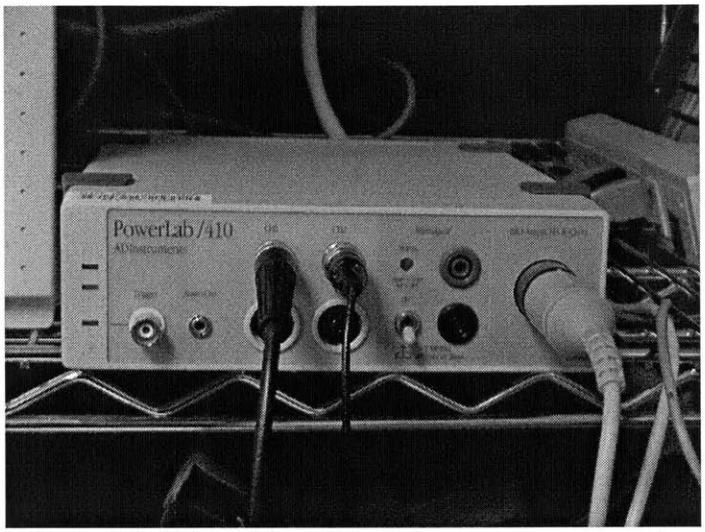

PowerLab 410, used for PPG vs. Pressure measurements

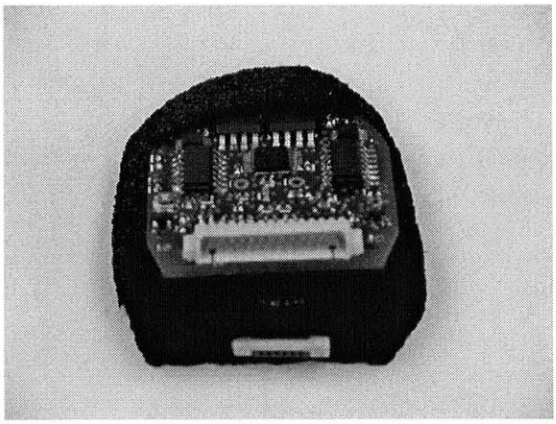

Processing unit embedded in foam (protects components, hides wires)

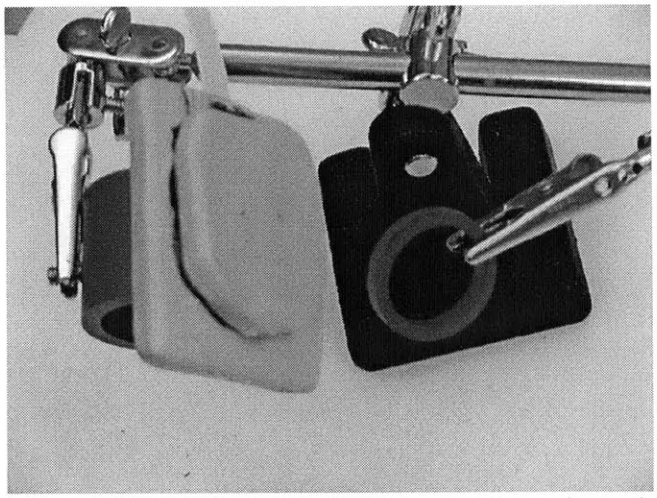

Full Assembly of Ring Sensor Design and Processing unit

LOW-PASS BUTTERSWORTH FILTER

Circuit Design

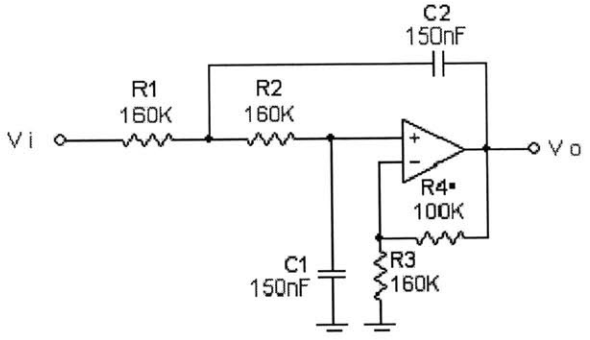

stage 1

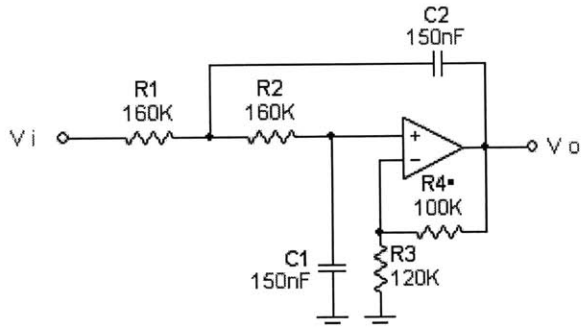

stage 2

Theoretical Response

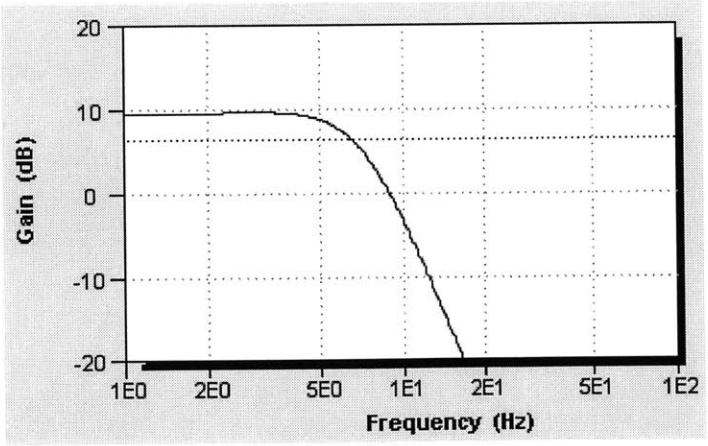

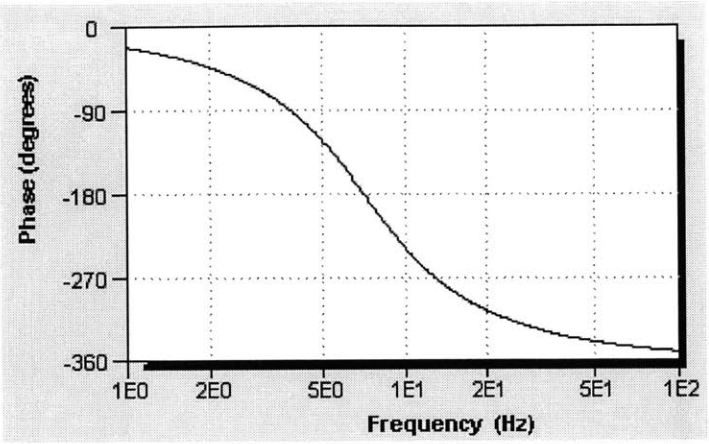

Experimental Response

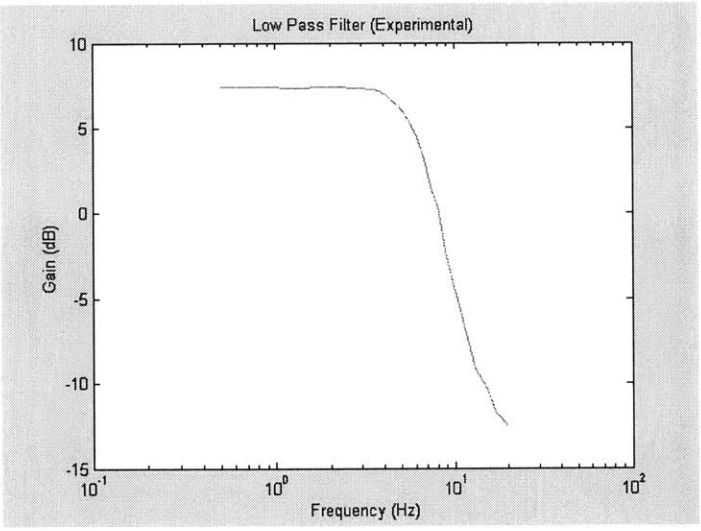

HIGH PASS BUTTERSWORTH FILTER

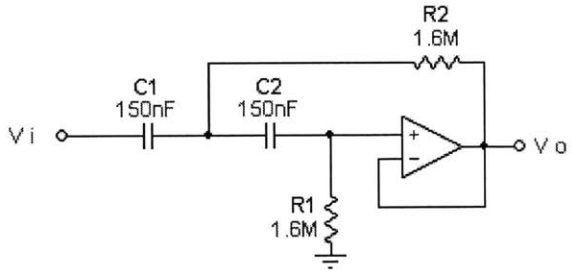

Theoretical Response

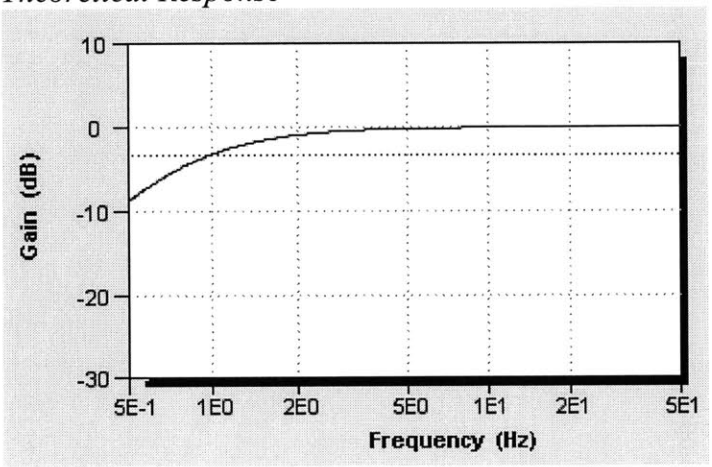

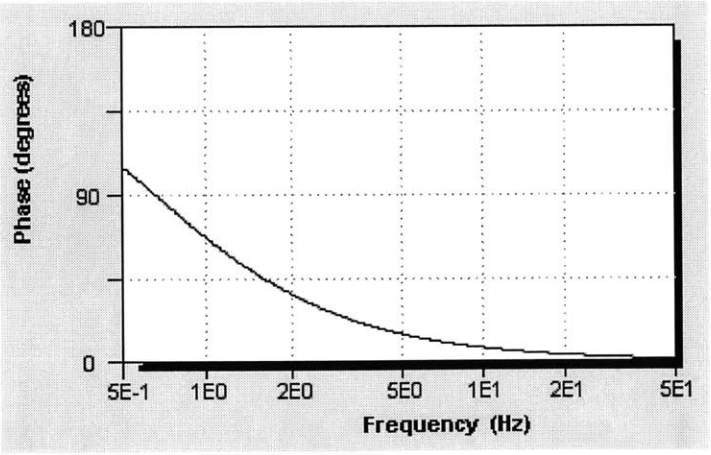

Experimental Response

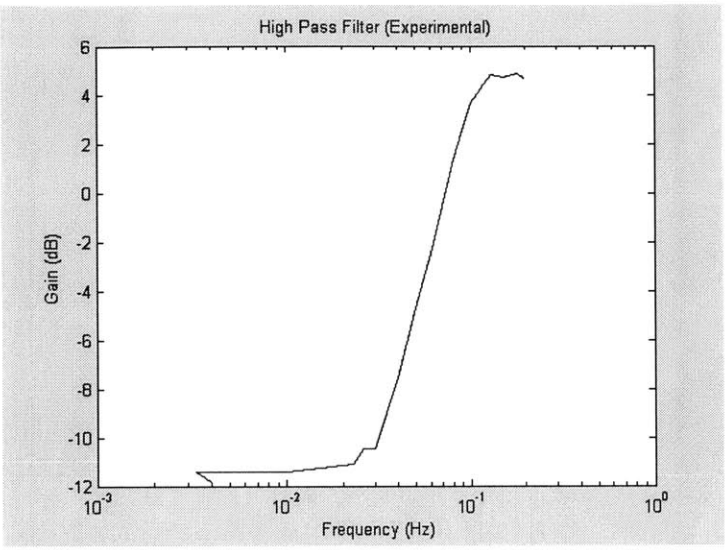

REFERENCES

[1] Barreto, A.B.; Vicente, L.M.; Persad, I.K., "Adaptive Cancellation of Motion Artifact in Photoplethysmyographic Blood Volume Pulse Measurements for Exercise Evaluation," *Engineering in Medicine and Biology Society,* IEEE 17th Annual Conference, Vol.: 2, pp.983 –984, 1995.

[2] Barreto, A.B.; Vicente, L.M; Taberner, A., "Adaptive Pre-Processing of Photoplethysmographic Blood Volume Pulse Measurements," *Biomedical Engineering Conference*, Proceedings of the 1996 Fifteenth Southern, pp.114-117, 1996.

[3] Barreto, A.B.; Vicente, L.M.; Taberner, A.M., "DSP Removal of Respiratory Trend in Photoplethysmographic Blood Volume Pulse Measurements," *Southeastcon '96. Bringing Together Education, Science and Technology*, Proceedings of the IEEE, pp.96 -98, 98a, 1996.

[4] Barbagelata, Melissa and Asada H., "Wireless Fingernail Sensor for Continuous Long Term Health Monitoring", MIT Home Automation and Healthcare Consortium Phase 3, Report 3-1, October 1, 2000.

[5] Drablein, David and Schmidt, Carl, "Spectrophotometric Studies XII. Observation of Circulation Blood in Vivo, and the Direct Determination of the Saturation of Hemoglobin in Arterial Blood," Physiological Society of Philadelphia, September 19, 1944, pp.69-83.

[6] Doebelin, Ernest, Measurement Systems Application and Design, New York, McGraw-Hill Book Company, pp. 295-305, 1975.

[7] Fisher, John W., "Random Signals and Linear Systems," Biomedical Signal and Image Processing, 2002.

[8] Fung, Y.C., Biomechanics Circulation Second Edition, Springer, New York, 1984.

[9] Goldstein B, Sanders J., "Skin response to repetitive mechanical stress: a new experimental model in pig" Arch Phys Med Rehabil 1998;79(3):265-72.

[10] Gottlieb, A.S. and Caro, F.G., "Providing Low-tech Assistive Equipment Through Home Care Services: The Massachusetts Assistive Equipment Demonstration." Technology and Disability, 13(1), (2001), 41-53.

[11] Guyton, Arthur, Textbook of Medical Physiology, W.B. Saunders Company, Philadelphia, 1981.

[12] Hayes, M.J. and P.R. Smith., "Quantitative Evaluation of Photoplethysmographic Artefact Reduction for Pulse Oximetry in Biomedical Sensors, Fibers and Optical Delivery Systems" 1999. Stockholm, Sweden: SPIE.

[13] Hayes, M. and Smith, P., "Artefact Reduction in Photoplethysmography" Optical Society of America, Nov. 1998, Vol. 37, No. 31.

[14] Langewouters, G.J., Zwart, A., Busse, R. and Wesseling, K.H., "Pressure-diameter relationships of segments of human finger arteries," Clinical Physics and Physiological Measurement, 1986, Vol. 7, No. 1, 43-55.

[15] Oppenheim A.V., and Verghese, G.C., "Random Variables, Optimal Hypothesis Tests, Likelihood Ratio, Neyman-Pearson Tests, Receiver Operating Characteristics", Communication, Control, and Signal Processing, 2001.

[16] Rhee, S. Yang B-H and Asada H., "Modeling of Finger Plethysmography for Wearable Sensors," 21st Annual International Conference of the IEEE Engineering in Medicine and Biology Society, Atlanta GA USA, Oct 13-16, 1999.

[17] Rhee, S. Yang B-H and Asada H., "Theoretical Evaluation of the Influence of Displacement on Finger Photoplethysmography for Wearable Health Monitoring Sensors," Symposium on Dynamics, Control, and Design of Biomechanical Systems ASME International Mechanical Engineering Congress and Exposition, Nashville, Tennessee, November 14-19, 1999.

[18] Rhee, S. Yang B-H and Asada H., "Design of a Artifact-Free Wearable Plethysmographic Sensor," 21st Annual International Conference of the IEEE Engineering in Medicine and Biology Society, Atlanta GA USA, Oct 13-16, 1999.

[19] Rhee, S., Yang, B-H and Asada, H., "Artifact-Resistant, Power-Efficient Design of Finger-Ring Plethysmographic Sensors" IEEE Transactions on Biomedical Engineering, 48 (7) (2001) pp 795-805.

[20] Schmidt, Robert and Thews, Gerhard (Eds.), Human Physiology, Springer-Verlag, Berlin, 1983

[21] Shimazu, H., Ito, H. and Yamakoshi, K., "Noninvasive method for estimating the mean capillary pressure and pre- and postcapillary resistance ratio in human fingers," Medical & Biological Engineering & Computing, 1986, 24,585-590.

[22] Stanley, A. G., *Present Status of Cadium Sulfide Thin Film Solar Cells*, 1967.

[23] Stedman's Medical Dictionary, 27th ed, Lippincott Williams & Wilkins, 2002.

[24] Tremper, K., Barker, S., Pulse Oximetry. Anesthesiology 70:98-108, 1989.

[25] Vaseghi, Saeed V.: Advanced Digital Signal Processing and Noise Reduction Second edition, John Wiley & Sons, LTD, Cichester, 2000.

[26] Tubiana, Raoul (ed), The HAND, W.B. Saunders Company, Philadelphia, vol. 1, 1981.

[27] Welch, DeCesare, and Hess, "Pulse Oximetry: Instrumentation and Clinical Applications," *Respiratory Care* 35:6:588, 1990.vv

[28] Wood, Earl, and Geraci, J.E., "Photoelectric Determination of Arterial Oxygen Saturation in Man," Section on Physiology, Mayo Clinic and Mayo Foundation, Nov. 15, 1948, pp. 387-401.

[28] Widrow, Benard, "Adaptive Noise Cancelling: Principles and Applications," Proceedings of the IEEE, vol 63, no.12, 1975, pp.1692-1719.

[29] Yamakoshi, K., Shimazu, H., and Togawa, T., "Indirect Measurement of Instantaneous Arterial Blood Pressure in the Human Finger by the Vascular Unloading Technique," IEEE Trans. on Biomed. Eng., Vol. 27, pp. 150-155, 1980

[30] Zijlstra, W. G., Buursma, A., and Meeuwsen-van der Roest, W. P., 1991. Absorption spectra of fetal and adult oxyhemoglobin, de-oxyhemoglobin, carboxyhemoglobin, and methemoglobin. *Clin. Chem.*, 37: 1633-1638.